

ABSTRACT

There have been many attempts by various researchers to utilize the Kaiser effect to determine in-situ stress in rocks. A thorough and foolproof technique would mean reduction in cost of in-situ stress determination as well as reduction of loss of material underground due to conservative safety factors.

This paper details the origin and the development and refinement of the Kaiser effect technique for determining in-situ stress in geologic structures. Since the analytical methods used to evaluate the Kaiser stress from the experimental data have an important bearing on the determined stress values, the available analytical procedures have been dealt in detail.

Literature shows that there exist two schools of thought in interpreting the Kaiser stress determined. The determined Kaiser stress might indicate the previous maximum stress or the current prevailing stress in the geologic structure. The literature available on both of these ideas has been presented in this paper. It is the author's opinion that the Kaiser stress indicates the previous maximum stress and it is with this conclusion, the entire Kaiser effect studies have been conducted.

Though many researchers have attempted to use the Kaiser effect for in-situ stress determination, the data they obtained is not very consistent with the fundamental principles of physics and mechanics. So, this paper attempts to put together the works of researchers on the theoretical principles behind the concept of the Kaiser effect. Since crack propagation is supposed to be the primary reason for the enormous acoustic

emission (AE) generated during the loading of a rock specimen, the theory of crack propagation has been dealt with in some detail. The opinion of researchers regarding whether the Kaiser effect can be utilized for determining in-situ stress in rocks has also been discussed.

The author had conducted tests to determine the pre-load stress in rock specimens using the Kaiser effect technique. The experimental procedure involved in these tests has been described in detail, starting from the preparation of specimens, pre-stressing of “master specimens”, coring of smaller specimens, end-capping of smaller specimens to the arrangements for the uniaxial reloading and acoustic emission data acquisition.

It’s the feeling of the author that uniaxial reloading of a triaxially pre-stressed rock specimen should depict the stress history because the AE onset stress is a function of all the three principal stresses that were acting on the rock.

TABLE OF CONTENTS

List of Figures	vii
List of Tables	ix
Acknowledgments	x
CHAPTER 1. Introduction	1
CHAPTER 2. Acoustic Emission Concepts	4
2.1 AE Parameters	5
2.2 Laboratory Monitoring Systems	7
2.2.1 Laboratory Transducers	8
2.2.2 Monitoring Facilities	9
CHAPTER 3. History of Kaiser Effect Studies	14
3.1 Origin of the Kaiser Effect	14
3.2 Goodman's Results	15
3.3 Kanagawa's Findings	16
CHAPTER 4. Kaiser Effect Method's Ambiguities	19
4.1 Methods of Evaluating Kaiser Stress from Experimental Data	19
4.1.1 Methods of Tangents	19
4.1.2 Maximum Curvature Method	19
4.1.3 Difference Method	20
4.1.4 Felicity Ratio Profile	20
4.1.5 Regression Analysis	21
4.1.6 Pivot Point Method	22

4.2 Prevailing Stress or Previous Maximum Stress?	23
4.3 Uniaxial Reloading of Rock Core	26
CHAPTER 5. Theory of Kaiser Effect	28
5.1 Crack Growth in Compression	28
5.2 Kaiser Effect Mechanism based on the Fracture Model	31
CHAPTER 6. Development of Standard Test Procedure	37
6.1 Test Material	37
6.2 Specimen Preparation	38
6.2.1 Coring	39
6.2.2 Cutting	41
6.2.3 Surface Grinding	43
6.2.4 End-Cap Installation	43
6.2.5 Lathe Operations	47
6.3 Pre-Stressing of Master Specimens	49
6.3.1 Triaxial Pre-Stressing of Master Specimens	49
6.3.2 Uniaxial Pre-Stressing of Master Specimens	54
CHAPTER 7. Discussion	56
References	58

LIST OF FIGURES

Figure	Page	
2.1	Typical section of AE data and an expanded AE event (After Hardy ¹⁰)	5
2.2	Basic construction of a simple AE transducer (After Hardy ¹⁰)	9
2.3	General view and dimensions of the Dunegan/Endevco model D-140B AE transducer	9
2.4	Single-Channel AE monitoring facility	10
2.5	Pulse output from a threshold detector in response to an incoming AE event (After Hardy ⁸)	11
2.6	Format of a typical Digital Counter (After Hardy ⁸)	12
2.7	Block diagram of a parameter development module for generating accumulated (total) count data (After Hardy ⁸)	12
2.8	Block diagram of a parameter development module for generating count rate data (After Hardy ⁸)	13
3.1	A Simple laboratory arrangement and typical data associated with Kaiser effect tests (After Zelanko ³⁴)	15
3.2	Shape of special specimen developed for Kaiser effect studies (After Kanagawa ¹⁸)	18
3.3	Typical Kaiser effect laboratory data and comparison of stresses from laboratory and field tests (After Kanagawa ¹⁸)	18
4.1	AE activity for previous loading, the first and second reloading and Stress as a function of time (After Yoshikawa ³³)	20
4.2	AE/MS incremental counts vs. stress for Indiana Limestone, Uniaxially preloaded	21
4.3	Pivot point method applied for determining Kaiser stress using Total and incremental count methods (After Hardy ¹¹)	22
4.4	Kaiser effect in mudstone after being subjected to repetitive loading (After Michihiro ²⁶)	24

4.5	Kaiser effect in specimens with strain recovered after axial stress Reduction (After Michihiro ²⁶)	25
4.6	A Situation where uniaxial reloading would not determine the in-situ stress in the loading direction	27
5.1	Crack growth in compression (After Brace ³)	29
5.2	Result of actual crack growth in photo-elastic plastic (After Brace ⁴)	29
5.3	Simplified crack model (After Li ²²)	30
5.4	Sketches showing the fracture and AE under uniaxial loading and reloading (After Li ²³)	31
5.5	Wing cracks induced by loading and reloading in different directions (After Li ²³)	32
5.6	Biaxial Loading (After Li ²³)	34
5.7	Ideal AE record under uniaxial reloading of a biaxially preloaded specimen	35
6.1	Preparation of cores using a diamond drill	40
6.2	Diamond saws used for cutting of master and smaller specimens	42
6.3	Overall view of surface grinder set-up	44
6.4	Details associated with end-cap installation	46
6.5	Specimen located in lathe, ready for grinding	48
6.6	Rock specimen with end-caps showing dimensions	48
6.7	Loading arrangement for triaxial pre-stressing of master specimens	51
6.8	Triaxial cell and master specimen	52
6.9	Plumbing arrangement to provide confining pressure during triaxial pre-stressing of master specimens	53
6.10	Loading arrangement for uniaxial pre-stressing of master specimens	55

LIST OF TABLES

Table		Page
4.1	Comparison of stress data obtained by Kaiser, Overcoring and Finite Element methods (After Hayashi ¹²)	23
6.1	Physical properties of Indiana Limestone and Cordova Limestone	38
6.2	Axial stress and Confining pressure combinations for triaxial Pre-stressing	49

CHAPTER 1

INTRODUCTION

For many years researchers have been interested in developing techniques to provide information on the state of stress in geological structures. In particular, knowledge of the in-situ stress states is of great importance in mining and geotechnical engineering applications. This information is useful in achieving a safe design for underground structures; evaluating the current stability of structures like deep tunnels and underground power stations; investigating the geologic activity of faults; evaluation of the stability of underground structures; and to provide data for the prediction of collapse or failure of underground openings. In general, the state of stress is a controlling factor in determining the size and spacing of openings underground; and increasing the extraction ratio and thereby reducing the production costs. The effect of surrounding geological formations on an underground structure needs to be investigated for design and installation of temporary or permanent supports. A thorough knowledge of the in-situ stress field would, therefore, help in reducing the sometimes-exaggerated safety factors utilized.

It is generally true that a rock mass is in a state of stress equilibrium. Stresses are redistributed when an excavation is created. At the surface of the opening, the normal stresses are reduced to zero and stress concentrations occur in the vicinity of the excavations. As a result, the available energy is stored in the form of elastic strain energy in the surrounding rock mass. Rock bursts, which are violent failure of the rock structure accompanied by the release of the energy and noise, occur at points of very high stress concentration. These rock bursts could be prevented by suitable stress-relief or

reinforcement techniques. However, these techniques require an understanding of the overall stress state in the rock mass.

There is a wide range of techniques available to determine in-situ stresses. Most of the conventional in-situ stress measurement techniques, like the over-coring technique, flat jack method, borehole strain cell method etc. involve determining the stress in-situ and are generally expensive as well as time consuming (Haimson, 1974, Leeman, 1969, Leeman and Hayes, 1966, Obert and Duvall, 1967). Therefore, there is a need for other methods of in-situ stress determination that could be performed in the laboratory on rock cores extracted from the geologic structures. One such method that could be performed in the laboratory and is less expensive and easy to apply is the method that utilizes the acoustic emission (AE) principle called the “Kaiser effect”.

It has been generally accepted that rocks, when stressed, emit sub-audible noises. This phenomenon is called Acoustic Emission (AE). The Kaiser effect can be defined as the absence of AE at stress levels below a previously applied maximum stress. In-situ stress determination using the Kaiser effect involves laboratory AE tests on rock cores retrieved from the geological structure under investigation. The AE-onset stress while loading the rock core was considered to be the stress the rock was under, in-situ, in the direction of loading in the laboratory. In the past, researchers have been reloading specimens cored from the three principal stress directions to obtain the principal stresses. This is possible only if the AE effects in the three principal stresses could be “de-linked”. At present, no satisfactory method for separating the stress components has been developed. Therefore, the concept that the uniaxial reloading of a rock specimen would directly yield the in-situ stress in the reloading direction may be erroneous in at least

some cases. Researchers have proved that during the uniaxial reloading in the direction of the major principal stress of a biaxially pre-stressed rock specimen, the AE-onset stress (Kaiser stress) was not the major principal stress. This paper outlines the various steps involved in investigating the relationship between the AE-onset stress and the previously applied stress. Li (1998) carried out a related study and also developed some related mathematical equations. However, he considered only the uniaxial reloading of the rock specimens in the direction of the major principal stress. In this current paper, some preliminary studies, initiated in order to study the above problems, were undertaken. Here smaller specimens, cored from triaxially pre-stressed “master” specimens at angles of 0° , 45° , 60° and 90° , were uniaxially reloaded allowing the problem to be investigated in a more general manner. Procedures for specimen preparation and testing are included in this paper. To date only a limited number of tests were carried out.

CHAPTER 2

ACOUSTIC EMISSION CONCEPTS

It is generally accepted that most solids, when stressed, emit sub-audible noises or low-level seismic signals. There are a variety of terms to describe the phenomenon, including acoustic emission (AE), micro-seismic (MS) activity, seismo-acoustic activity, rock noise, stress wave analysis technique (SWAT), elastic shocks, and elastic radiation. However, in this thesis, this phenomenon will be referred to as acoustic emission.

In geologic materials, the origin of acoustic emission is not very clearly understood, but it appears to be related to the process of deformation and failure which are accompanied by a sudden release of strain energy (Hardy, 1981). In geologic materials, which are mainly polycrystalline in nature, AE may originate at the micro-level as a result of dislocations, or at the macro-level by twinning, grain boundary movement, or initiation and propagation of fractures through and between mineral grains. It is assumed that the sudden release of stored elastic strain energy accompanying these processes generates an elastic stress wave, which travels from the point of origin within the material, to a boundary where it is observed as AE.

In recent years, the application of AE techniques in geotechnical engineering has rapidly increased. This technique has been used for stability monitoring in mines, petroleum and natural gas caverns, radioactive waste repositories, and geothermal reservoirs. AE techniques are increasingly being used in laboratory-scale studies of both, basic and applied nature. Hardy (1989) provides a detailed review of a wide range of

geotechnical AE applications. The following sections discuss the AE concept, monitoring techniques, and the Kaiser effect.

2.1 AE Parameters

A variety of parameters are used to describe AE signals observed during laboratory and field AE studies. In most of the laboratory AE studies, the AE signals themselves are not recorded, rather, these signals are processed on-line using analog or digital techniques to provide various parameters like, event rate or energy rate.

Figure 2.1 illustrates a typical section of AE data and an expanded AE event. According to Hardy (1992) in the time domain such data is commonly described in terms of the following parameters:

- (1) Accumulated Activity (N): The total number of events observed during a specific period of time.

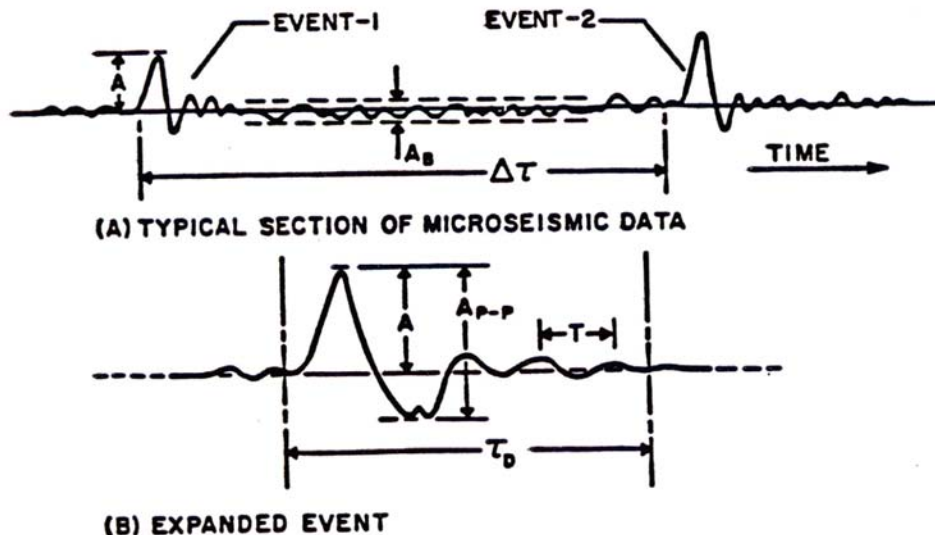


Figure 2.1 Typical Section of AE Data and an Expanded AE Event (After Hardy, 1992).

- (2) Event Rate (NR): The number of events (ΔN) observed per unit time (Δt).
- (3) Amplitude (A): The peak (maximum) value of each recorded event.
- (4) Peak-to-Peak Amplitude (A_{p-p}): The amplitude measured between the maximum positive and negative peaks of the event.
- (5) Background Amplitude (A_B): The signal level present in the absence of well-defined events. A_B as shown in Figure 2.1 is actually the peak-to-peak background amplitude.
- (6) Signal + Noise-to-Noise Ratio (SNR): The ratio of the event plus background amplitude to the background amplitude.
- (7) Energy (E): The square of the event amplitude (A).
- (8) Accumulated Energy (ΣE): The sum of the energy emitted by all events observed during a specific period of time.
- (9) Energy Rate (ER): The sum of energy emitted by all events observed per unit time (Δt).
- (10) Period (T): The time between two successive peaks of the event.
- (11) Average Fundamental Frequency (f): The reciprocal of the average period computed over n cycles of the event.
- (12) Event Duration (τ_D): The total time of occurrence for an individual event.
- (13) Time-Between-Events ($\Delta\tau$): The time between successive events, i.e., the time between the beginning of one event and the beginning of the next.

2.2 Laboratory Monitoring Systems

AE laboratory studies involve the detection and processing of events occurring in a finite body (specimen or model). This is very much in contrast to the field AE studies where infinite or semi-infinite bodies are often involved. The major differences between AE laboratory and field studies are the smaller source dimensions, the finite nature of the structure under study and shorter source-to-transducer distances. Hence, the data detected during laboratory AE studies generally exhibits the following characteristics:

- (1) high dominant signal frequencies,
- (2) low signal amplitudes,
- (3) high event rates, and
- (4) signal complexities due to stress wave reflection from specimen or model boundaries.

The finite nature of the specimen in laboratory AE studies has advantages as well as disadvantages. Since the specimen generally consists of a single type of material, the wave propagation complexities due to reflection and refraction within the specimen itself, is eliminated. However, it may give rise to problems due to reflections at free boundaries and at specimen-test fixture interfaces. Care must also be taken with respect to the resonant frequencies of the structure and the associated test fixtures, and also the effect of the transducer on these frequencies. A number of studies have indicated that the frequency spectra of AE events detected in laboratory structures do reflect these intrinsic resonant frequencies, at least to a limited degree.

2.2.1 Laboratory Transducers - Most AE laboratory studies in the geotechnical area involve the detection of events with dominant frequencies in the range 50 kHz – 500 kHz. However, the common range based on the availability of commercial transducers, which include accelerometers, AE-transducers and piezoelectric elements, is 100 kHz – 300 kHz. In the current study, AE-transducers were utilized and only this type will be discussed here.

AE-transducers have become commercially available in the last 25 years. Such transducers consist of a single piezoelectric disc mounted on a flat sole or wear-plate and contained within a suitable protective housing (Figure 2.2). In use the transducer is attached to the structure under study. An AE wave striking the wear plate induces a stress within the piezoelectric disc that generates an equivalent output voltage. Most of the AE-transducers are used in the resonant mode to achieve higher sensitivity. However, a number of transducers with a “flat frequency response” over a somewhat extended frequency range are also available.

AE-transducers are supplied by manufacturers in two forms, namely the single-ended and differential form. The differential form of AE-transducer, due to its more complex piezoelectric element configuration, can be utilized with a suitable differentiable pre-amplifier to cancel out electrical noises. This increases the effective signal-to-noise ratio (SNR) of the overall monitoring system. Figure 2.3 illustrates a commonly used Dunegan/Endevco model D-140B AE-transducer of the resonant type. The prefix “D” indicates that the transducer is of differential form.

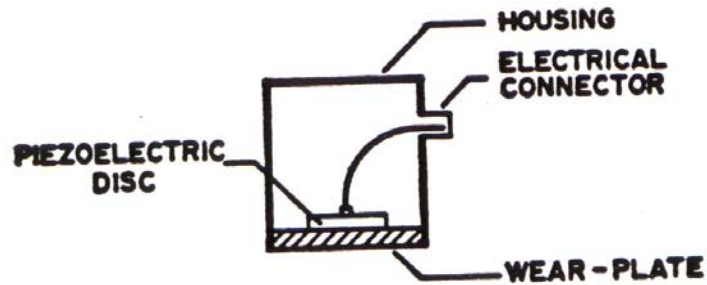


Figure 2.2 Basic Construction of a Simple AE-Transducer (After Hardy, 1992)

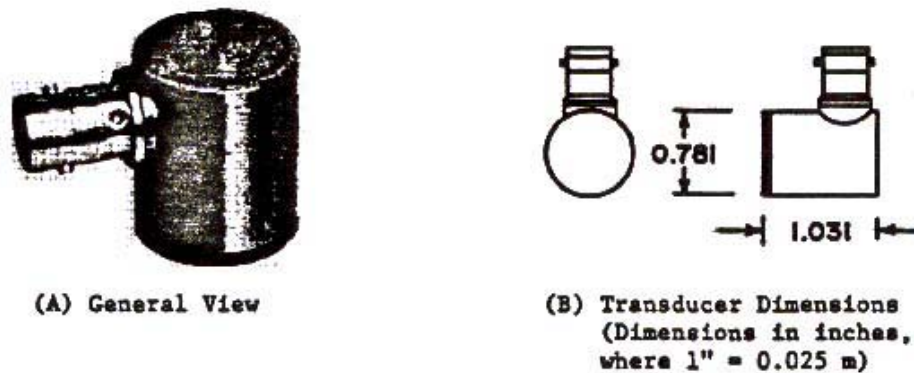


Figure 2.3 General View and Dimensions of the Dunegan/Endevco Model D-140B AE-Transducer

2.2.2 Monitoring Facilities - The monitoring system used in the current study is of the single-channel parametric type. Figure 2.4 shows a block diagram of one such system. The major disadvantage of a parametric system is that the detailed character of the AE signals is lost, however, such a system is capable of conveniently processing the large number of high frequency signals normally encountered in laboratory studies in geologic materials.

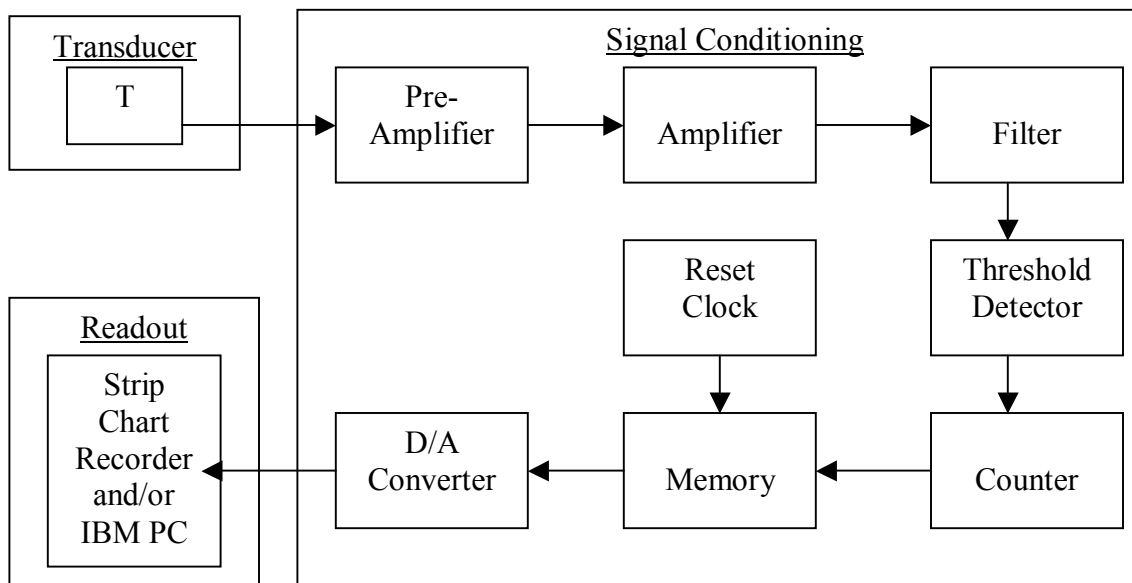


Figure 2.4. Single-Channel AE Monitoring Facility (After Hardy, 1992).

The parameter development section of the monitoring facility consists of a number of elements combined to provide the desired AE parameters, like threshold detector, digital counter, count rate module, accumulated counts module, etc. which are briefly described below.

1. Threshold Detector – The Purpose of the threshold detector is to convert analog AE signals to a pulse format. Figure 2.5 illustrates an incoming analog signal and the equivalent pulse output based on a threshold level of ΔV . The threshold detector usually is a form of Schmidt trigger circuit, which produces a square pulse of fixed amplitude and duration each time the incoming signal exceeds a specific voltage level, denoted as the threshold level.

As depicted in Figure 2.5 the incoming signal exceeds the threshold level (ΔV) three times (points 1, 3 and 5) during the duration of the event (ΔT). At each of these

times, a pulse is generated at the output of the threshold detector. These are known as ‘ring-down’ pulses. It should also be noted that Figure 2.5 depicts a case of a single AE event generating three ring-down pulses. In general, AE activity may therefore be defined in terms of event counts (N_E) or the number of ring-down counts (N_{RD}). This presents a certain degree of ambiguity since the relationships between N_{RD} and N_E will depend on the amplitude of the incoming event and the selected threshold level.

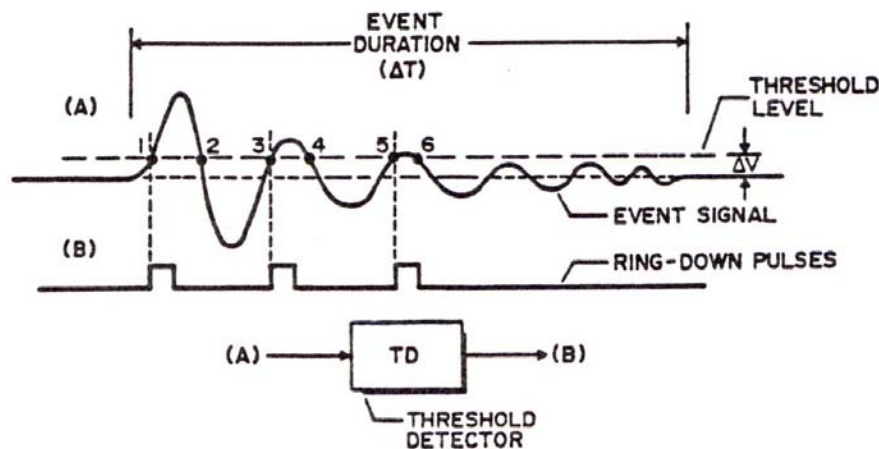


Figure 2.5 Pulse Output from a Threshold Detector in Response to an Incoming AE Event. [(A) – Incoming AE Event, (B) – Pulse Output.] (After Hardy, 1985).

2. Digital Counter – The function of a digital counter is to accept the incoming pulses from the threshold detector, count, totalize and store these, and provide a suitable output. As illustrated in Figure 2.6, stored data may be displayed visually using accessory elements, and such counters are usually equipped with circuits to provide start, stop and reset (storage dump) functions.

3. Total (Accumulated) Counts Module – The parameter development module for generating total count data is depicted in Figure 2.7. Here pulses generated by the threshold detector, in response to the AE analog input signal, are fed into a counter. The

output of the counter is a digital signal equivalent to the total number of counts accumulated.

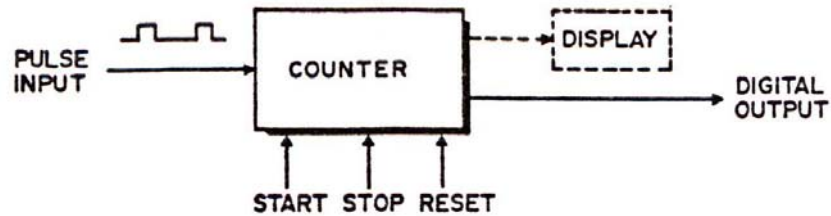


Figure 2.6. Format of a Typical Digital Counter (After Hardy, 1985).

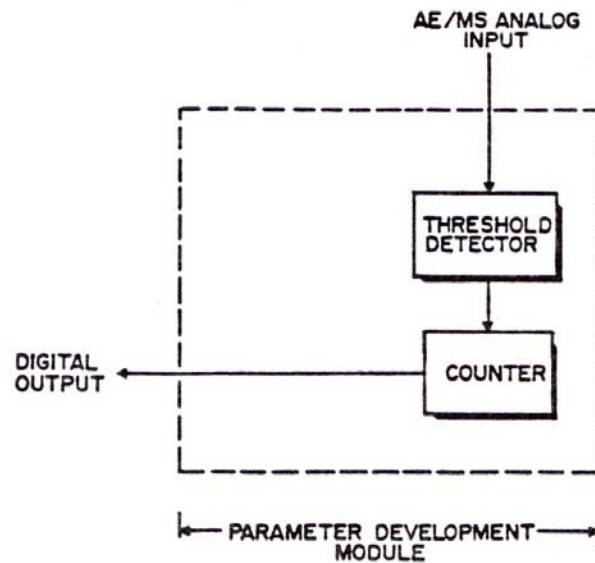


Figure 2.7. Block Diagram of a Parameter Development Module for Generating Total (Accumulated) Count Data (After Hardy, 1985).

4. Count Rate Module – The total counts module is slightly modified with an addition of a reset clock to generate the count rate data (Figure 2.8). The function of the reset clock is to provide a reset pulse to the counter at selected intervals of time. In operation, pulses generated by the threshold detector, in response to the incoming signals, are fed into the counter and accumulate until the clock generates a reset pulse. This

dumps the counter, dropping the digital output to zero, and initiating a new count sequence. The equivalent count rate of such a system is equal to the total number of counts accumulated between reset pulses divided by the time between such pulses.

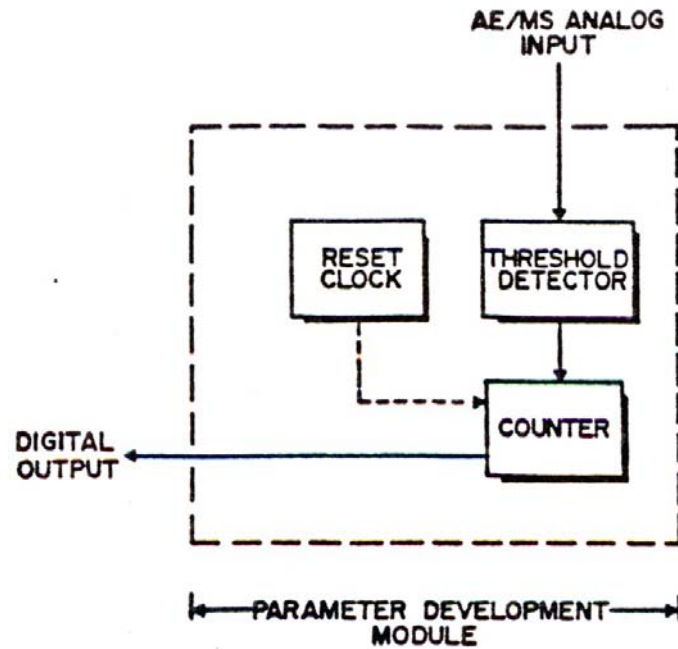


Figure 2.8. Block Diagram of a Parameter Development Module for Generating Count Rate Data (After Hardy, 1985).

CHAPTER 3

HISTORY OF KAISER EFFECT STUDIES

3.1 Origin of the Kaiser Effect

Josef Kaiser (1953), a Germany researcher was the first person to observe the phenomenon that now, bears his name. The discovery was made during a study of the AE response of metals in the early 50's. Kaiser indicated that metals retain a memory of the previously applied stress field.

The Kaiser effect can best be described by considering a simple experiment in which the phenomenon is evident. Consider, for example, a laboratory set-up as shown in Figure 3.1(a) in which a rock specimen is subjected to two cycles of loading. In the first load cycle, stress is applied to the specimen at a constant rate up to a value of σ_{\max} (see Figure 3.1(b)) and then returned to zero. In the second cycle, stress is increased in a similar fashion, however, the previous maximum stress σ_{\max} is exceeded. During each cycle, AE activity is monitored by a system that is capable of detecting AE events and recording them cumulatively.

Figure 3.1(b) represents data, which is typical of such an experiment. This figure shows the cumulative number of AE events generated by the specimen during each of the two load cycles. It can be seen that AE is generated at all stress levels during the first loading cycle. During the second cycle, however, no AE is generated until the stress level attained in the first load cycle is exceeded. Thus, the Kaiser effect can be defined as the absence of AE at stress levels below a previously applied maximum stress.

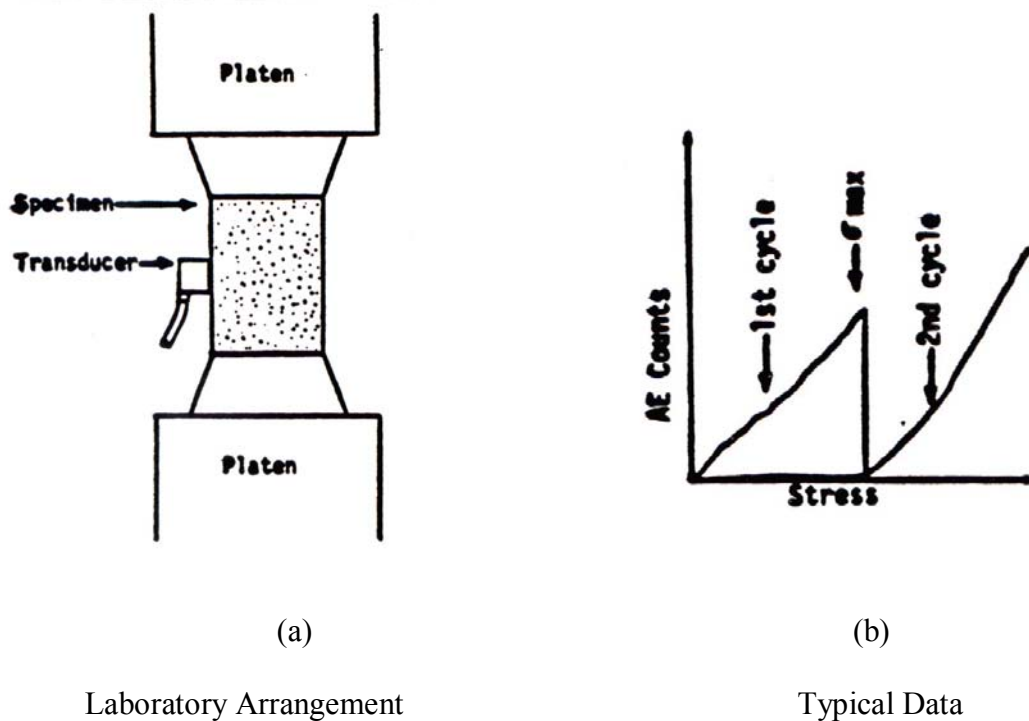


Figure 3.1 A Simple Laboratory Arrangement and Typical Data Associated with Kaiser Effect Tests (After Zelanko, 1983).

3.2 Goodman's Results

One of the first reported studies of the Kaiser effect in rock appears to have been carried out by Goodman (1963). In this study, Goodman investigated the effect of cyclic uniaxial compressive loading on the AE response of specimens of sandstone and quartz diorite. Goodman observed a distinct pattern of response in the detected AE activity and classified it into three types, namely:

Type 1 – AE events at low stress levels which disappear with numerous repetitions of load

Type 2 – AE events at low stress levels which persist despite load repetitions,
and

Type 3 – AE events at high stress levels, which occur more frequently upon repetition of load.

Goodman reported that the Type 1 activity disappeared after repetitions of load (indicative of the Kaiser effect) and also observed that this type of activity appeared to reappear after a previously loaded specimen remained unloaded for a period of time. This particular observation, namely the decay of the Kaiser effect, diminished the researchers' interests in Kaiser effect for some years.

3.3 Kanagawa's Findings

Some 10 years later, Kanagawa et al. (1976) conducted a series of very well organized studies on the use of AE measurements, and application of the Kaiser effect for determining in-situ stress. They hypothesized that, if a rock core is removed from its in-situ stress state and reloaded in the laboratory, AE activity observed during the reloading cycle should exhibit the Kaiser effect. In essence, AE activity below the in-situ stress level should be minimal but above this level, AE activity should increase significantly. Kanagawa et al. (1976) postulated that the in-situ stress for a given rock core could be determined by noting the stress level at which the AE/MS activity begins to increase during uniaxial reloading. Furthermore, they speculated that the directional components of the in-situ stress field in a rock mass could be determined by testing a number of cores drilled at various orientations within the rock mass.

In their preliminary investigations, Kanagawa et al. (1976) developed specimen preparation procedures that could reduce the number of anomalous AE events generated at the ends of the specimen during loading. These events are usually caused by friction and stress concentrations at the contacts between the loading machine platens and the specimen ends. Stress concentrations at small irregularities at the specimen ends may also

give rise to considerable AE even at low stress levels. In order to reduce the “end-noise”, various materials were inserted between the loading platens and the specimen ends. It was concluded that the use of a so-called bonded “hunch” or end-caps located at each end of the specimen was the most effective means of reducing end-noise. A mixture of 1:1.5 (weight ratio) of Araldite epoxy and dry cement was found to be the most suitable end-cap material. Figure 3.2 illustrates the form of a typical “low-noise” specimen.

Kanagawa et al. (1976), then, developed standard testing and data analysis procedures. Test specimens were cut from sections of tuff rock core at various orientations. Prepared specimens, with AE attached transducers, were loaded at a constant rate, and load and total AE counts were recorded as a function of time. Two straight lines were then fitted to the AE curve, and the previous maximum load (in-situ stress) was determined by projecting the point of intersection of the two straight lines from AE curve onto the load curve (Figure 3.3A). To determine the accuracy of their method, Kanagawa et al. (1976) subjected several tuff specimens to known pre-load cycles. The results indicated that the Kaiser effect technique was accurate to within 15%. AE stress determinations were done on 11 different tuff specimens cored in various orientations. The overall results were then compared with the stress values obtained from over-coring type stress measurements carried out in the field (Figure 3.3B). Kanagawa et al. (1976) considered that stresses estimated by the Kaiser method were consistently higher than the stresses measured by over-coring and postulated that the Kaiser method may actually provide data on the historical maximum stress rather than current in-situ stress.

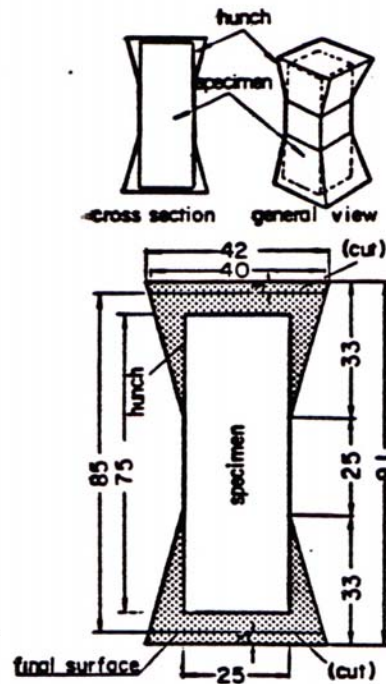
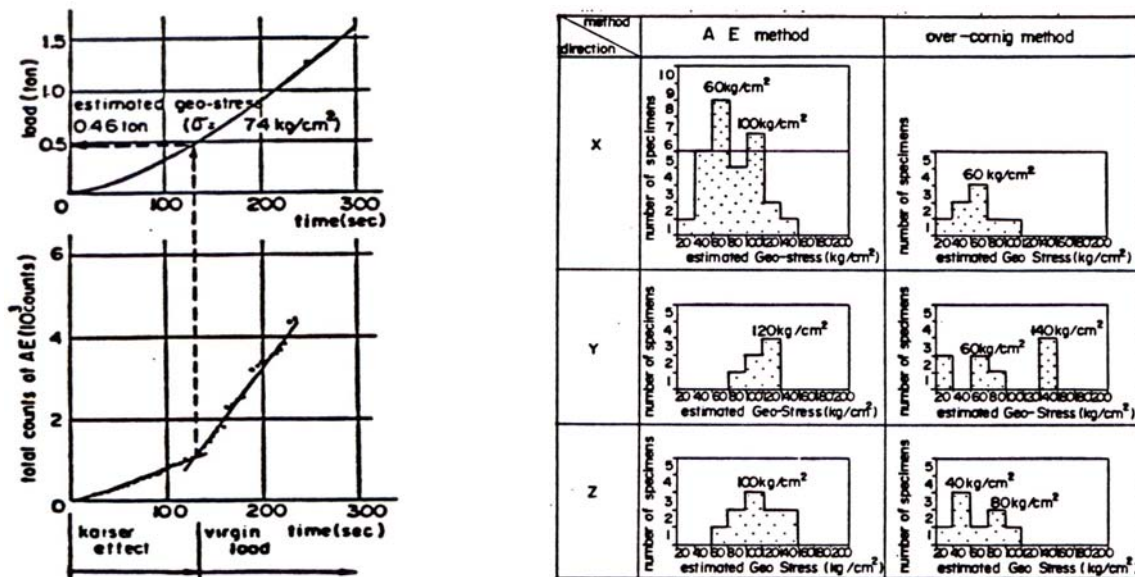


Figure 3.2 Shape of Special Specimen Developed for Kaiser Effect Studies (After Kanagawa et al. 1976). [Dimensions are given in millimeters]



(A) Typical Laboratory Data for Tuff (B) Comparison of Stresses Determined from Kaiser (AE) Method and Field Over-coring
 Figure 3.3 Typical Kaiser Effect Laboratory Data and Comparison of Stresses from Laboratory and Field Tests (After Kanagawa et al. 1976).

CHAPTER 4

KAISER EFFECT METHOD'S AMBIGUITIES

4.1 Methods of Evaluating Kaiser Stress from Experimental Data

Utilization of the Kaiser effect as a means of determining in-situ stresses in a geo-technical structure involves laboratory tests on cores retrieved from the structure. A review of the literature (Hardy 1989, 1995) clearly indicates that the Kaiser stresses determined from such tests will be highly dependent on the experimental and analytical procedure utilized. In this regard there are a variety of methods that have been used by various workers to determine the Kaiser stress from the experimental data. A number of these methods will be discussed in the following sections.

4.1.1 Method of Tangents - Boyce (1981) utilized an objective procedure to determine the Kaiser stress from the experimental data. Here, tangents were drawn to the early “quiet”, as well as the later more active portions of the AE versus applied stress data. The intersection of these tangents was then used to define the required Kaiser stress value.

4.1.2 Maximum Curvature Method - Momeyez et al (1992) utilized a method that determines the change in the slope of the Cumulative Acoustic Emission (CAE) curve by calculating the amount of curvature along this curve. This change of slope is indicative of the effect of the previously applied load. The maximum value of the curvature corresponds to the deflection point, which was then used to determine the Kaiser stress.

4.1.3 Difference Method - Yoshikawa and Mogi (1981) suggested a method to determine Kaiser stress in those cases where the Kaiser effect could not be clearly observed by plotting the experimental data. They showed that in a second reloading cycle, the observed AE activity was different from that of the first reloading cycle (Figure 4.1). They suggested that since the difference between the observed AE activity of the two cycles increased markedly at the previous stress, the previous stress could be determined using this difference.

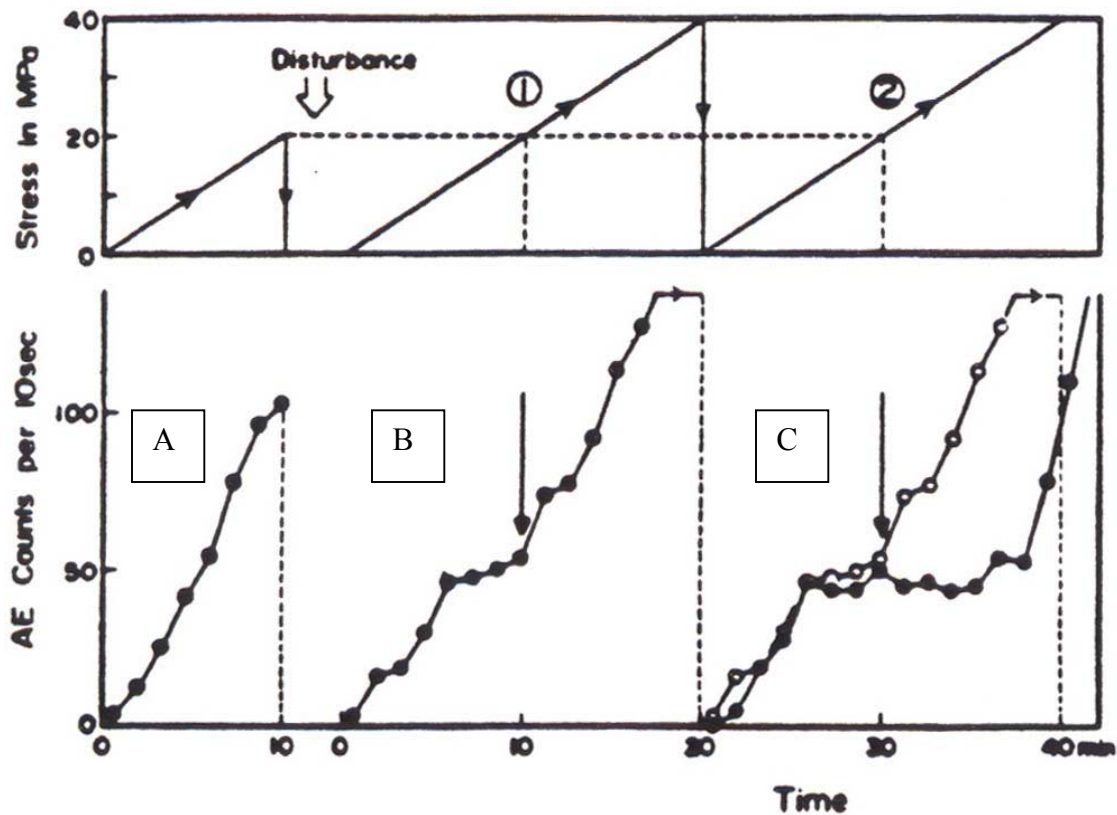


Figure 4.1 AE Activity for the Previous Loading (A), the First Reloading (B) and Second Reloading (C) and Stress as Function of Time (After Yoshikawa and Mogi, 1981). [In C, Open circles: AE Count Rate for First Reloading, Solid Circles: AE Count Rate for Second Reloading]

4.1.4 Felicity Ratio Profile - Hughson and Crawford (1986) used the felicity ratio profile to improve the estimates of stress using the Kaiser effect method. The felicity ratio is

defined as the ratio of stress estimated using acoustic emission to the known previous maximum stress. By determining the felicity ratio for a given material at different stress levels, a felicity ratio profile was generated. This profile was then used to improve the estimated Kaiser stress.

4.1.5 Regression Analysis - Hardy et al. (1985) utilized statistical analysis to fit lines to AE versus stress data and interpreted the intersection of the two lines as the Kaiser stress point. They utilized both the total count data as well as the incremental count data obtained from the experiments and plotted against the applied stress in the reload cycle. Linear regression techniques were then manually applied to the data and two lines L1 and L2 (see Figure 4.2) fitted to the data, below and above the apparent Kaiser stress level.

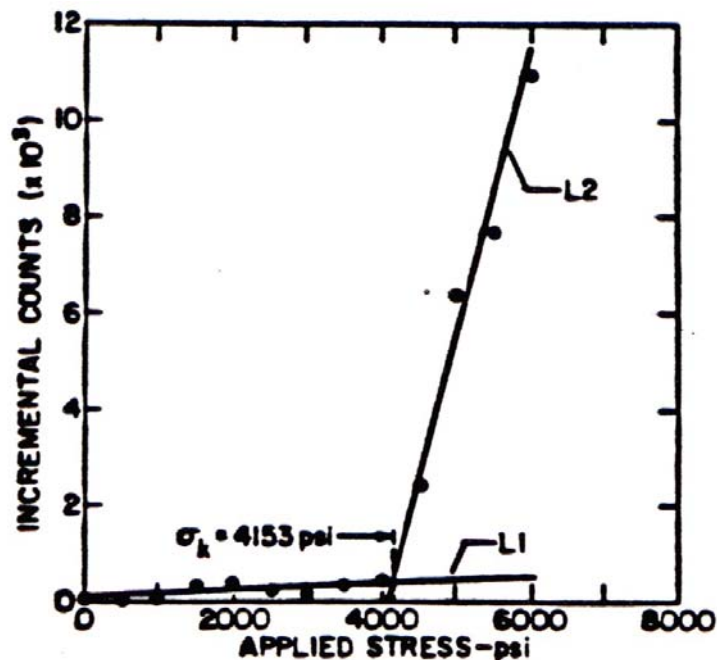


Figure 4.2 AE/MS Incremental Counts Vs Stress for Indiana Limestone Uniaxially Preloaded. Preload Stress = 4054 psi. Kaiser Stress = 4153 psi (After Hardy et al. 1985).

The intersection of lines L1 and L2 was then projected to the stress axis to define the Kaiser stress (σ_k). Similar analysis was later carried out using total AE count data and it was found that the results using incremental and total count data to be different. It was interpreted that total count data may be useful in those cases where the incremental count method is unsuitable.

4.1.6 Pivot Point Method - Hardy and Shen (1992) and Shen (1993) discuss the pivot point method to determine the Kaiser stress from the experimental data. In the method the total and incremental count data described earlier was used. It was emphasized that the starting point of the second regression line was very important relative to the accuracy in the determined Kaiser stress. In this regard they suggested that the point at which the

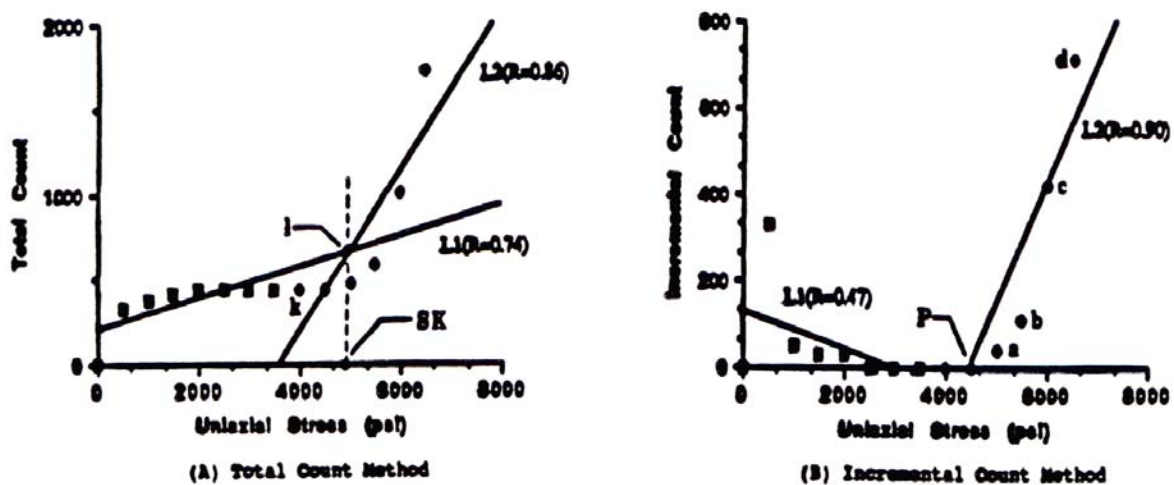


Figure 4.3 Pivot Point Method Applied for Determining Kaiser Stress Using Total and Incremental Count Methods (After Hardy and Shen, 1992).

incremental values of the incremental count data (or the total count data) starts to increase monotonously should be taken as the starting point of the second regression line. They denoted this point as the “Pivot Point” and showed that using this procedure the error in estimating Kaiser stress values was less than 4.0%.

4.2 Prevailing Stress or Previous Maximum Stress?

Hayashi (1979) attempted to use the Kaiser effect to determine in-situ stresses at the construction site of a nuclear power plant. At the construction site a slope, some 240-ft high was to be excavated. After excavation the in-situ stresses at a point below the newly excavated surface were determined both by over-coring method and Kaiser technique. The stresses at this point prior to and following the excavation were also determined using the Finite Element Method (FEM). The results are shown in table 4.1.

Stress Component	Stress – Kg/cm ² Before Excavation FEM	Stress - Kg/cm ² <u>After Excavation</u>		
		Kaiser	Overcoring	FEM
σ_x (Hor)	16	14-16	9	10
σ_y (Hor)	9	6-7	7	8
σ_z (Vert)	14	14-15	5	6

Table 4.1. Comparison of Stress Data Obtained by Kaiser, Over-coring and Finite Element Methods (After Hayashi, 1979).

It can be seen from the above table that the stresses determined by the Kaiser method after excavation compare favorably with those predicted by the FEM for the unexcavated slope where as the stresses measured by over-coring methods after excavation compare favorably with the FEM prediction for the excavated slope. These results show that the Kaiser method appears to provide stress data more closely associated with the stresses prior to excavation. However, they have failed to mention the time elapsed between the various stages of excavation. Experiments on soil specimens by Lord et al. (1985) for determining the pre-consolidation pressure using AE techniques have also yielded similar results.

Michihiro et al. (1985) performed Kaiser effect experiments on various kinds of rocks like tuff, mudstone etc. It has to be understood that rock in-situ has been subjected to the three principal stresses for a long time, and is in a saturated state of strain, that is, residual strain has been sufficiently generated that no further strain can be recognized under that



(a) Saturated Strain

(b) Unsaturated Strain

Figure 4.4. Kaiser effect in mudstone after being subjected to repetitive loading. (After Michihiro et al. 1989).

state of stress. Michihiro et al. (1989) suggest that Kaiser effect in rock depends on the condition of strains rather than the axial stress applied. (See Figure 4.4). Kaiser effect experiments on granite and tuff specimens by Michihiro et al. (1985) have shown that the stress estimated from the Kaiser effect is equal to the stress that presently causes strain in specimens rather than the largest stress they have sustained in the past. (See Figure 4.5).

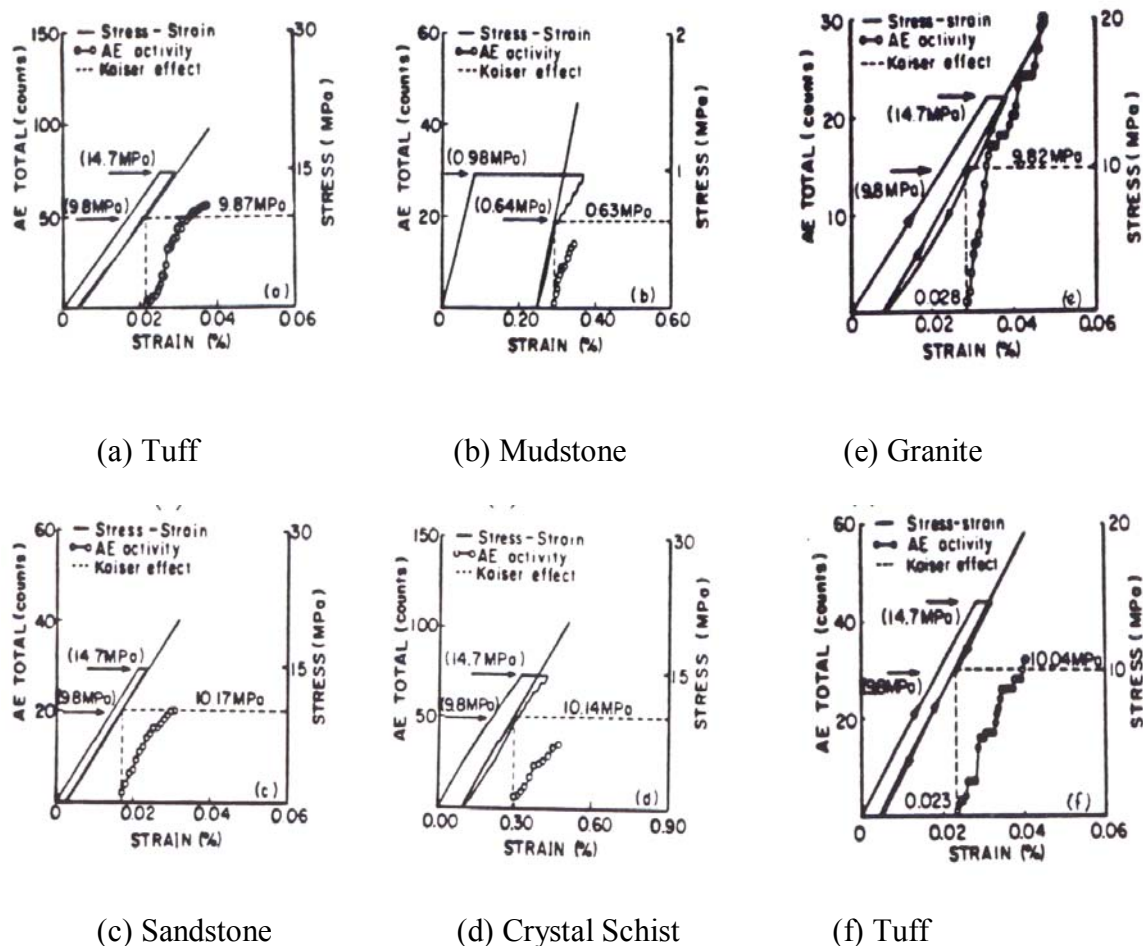


Figure 4.5. Kaiser Effect in Specimens with Strain Recovered after Axial Stress Reduction (After Michihiro et al. 1989).

They applied a constant stress of 14.7 MPa to granite specimens till the state of saturated strain was attained and after some time they brought down the stress level to 9.8 MPa and kept the stress at this level till saturated strain state was attained again. When they

reloaded the specimen uniaxially, the Kaiser stress was found to be 10.04 MPa. Similar results were obtained other rocks like tuff, sandstone, mudstone, and crystal schist.

4.3 Uniaxial Reloading of Rock Core

The technique of reloading a rock core extracted from its virgin state to determine the previous maximum stress in that direction may contain a basic fallacy. Consider a block of rock mass that has been acted upon by the three principal stresses. The assumed crack configuration in the rock mass is a small crack and a larger crack, with the larger crack representing the stress state and the angle between their orientations is say, 90° . Suppose a rock core is drilled out of the block and is reloaded uniaxially in a direction parallel to the smaller crack, there would be rapid increase in the observed AE due to the propagation of the smaller crack and not due to the larger one. The larger crack was assumed to be formed due to the application of the major principal stress and its interaction with the other principal stress. While reloading, the larger crack which represents the true original stress state, would start closing and not respond, where as, the smaller crack would start propagating and generate enormous AE and give a false image (See Figure 4.6). Since the rock mass is acted upon by all the three principal stress, the Kaiser stress obtained during reloading of the specimen should have a relationship with the in-situ stresses based on the fundamental principles of physics and mechanics. A lot of back-calculation is required to assess the situation.

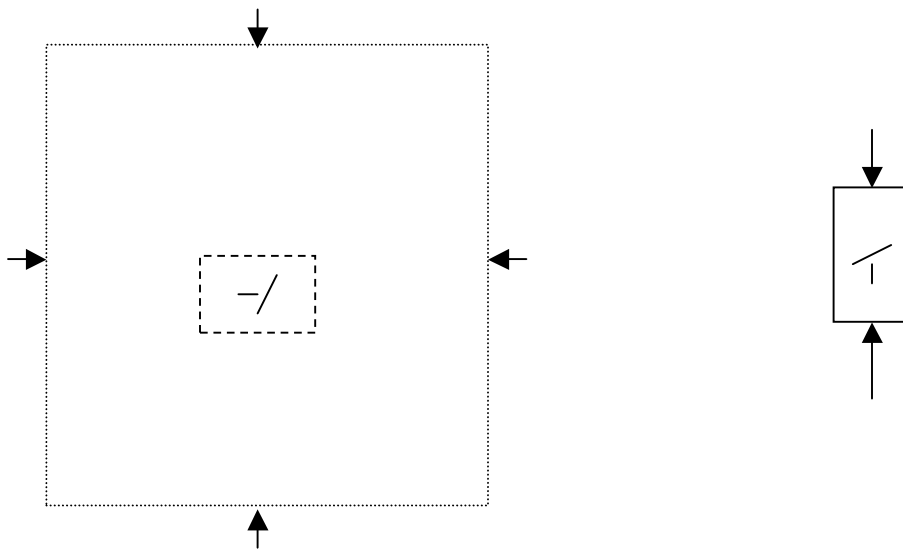


Figure 4.6. A Situation where Uniaxial Reloading would not determine the in-situ stress in the loading direction.

CHAPTER 5

THEORY OF THE KAISER EFFECT

Utilization of the Kaiser effect for determining in-situ stress necessitates that the mechanism by which rocks retain the memory of the earlier applied stress be understood. It is a well-known fact that rocks contain a large number of pre-existing cracks. Literature shows that there may exist two main sources for AE when a rock specimen is loaded in compression, namely, the frictional movement on the pre-existing crack surfaces, and the sudden advance of the crack tip (Kurita and Fujii, 1979). Sliding along crack surfaces accompanies the entire process of loading and forms the background AE. The fracture of intact material due to sudden crack tip advance commences only when the applied load reaches a certain critical level and results in generation of enormous AE activity. Therefore the Kaiser effect phenomenon should be studied in relation to the initiation and re-initiation of crack propagation in the rock specimen.

5.1 Crack Growth in Compression

Many researchers have studied the growth of cracks under compression (Brace and Bombolakis, 1963, Brace 1965). Their experimental results in model materials, as well as in rocks, clearly demonstrated that, under load, the newly initiated “wing cracks” tended to grow in the direction of the major principal compressive stress (Figure 5.1). In Bombolakis (1963) the crack growth was simulated and observed by a photo-elastic technique. It was observed that cracks always grew by the development of branch fractures that curved in the direction of applied compression. Brace and Bombolakis

(1963) also showed that crack growth occurred by extension of the initial crack along a curving path that gradually became parallel with the direction of compression. When this direction was attained, further crack growth stopped, apparently because of a decrease in tensile stress concentration at the tip of the branch crack.

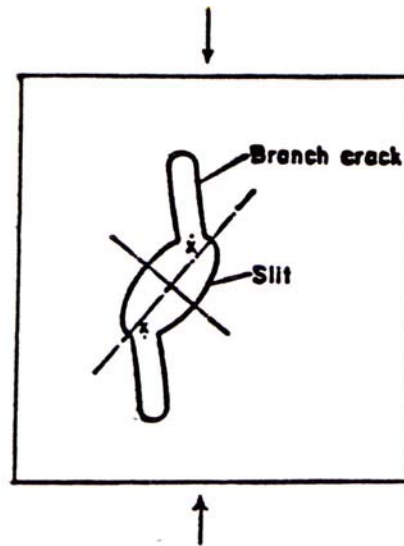


Figure 5.1. Crack Growth in Compression (After Brace and Bombolakis, 1963).

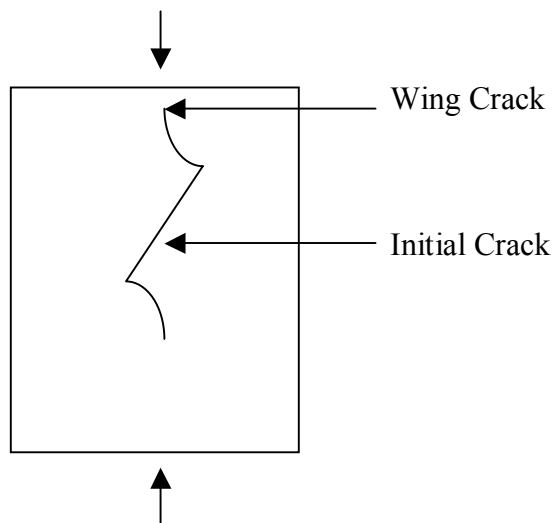


Figure 5.2. Result of Actual Crack Growth in Photo-Elastic Plastic (After Brace and Bombolakis, 1963).

It is assumed in these studies that the crack models that all the pre-existing cracks are open and have an elliptical shape and could be simplified to a crack loaded by a central wedge force F (per unit thickness of the plate) in the direction of σ_2 (see Figure 5.3).

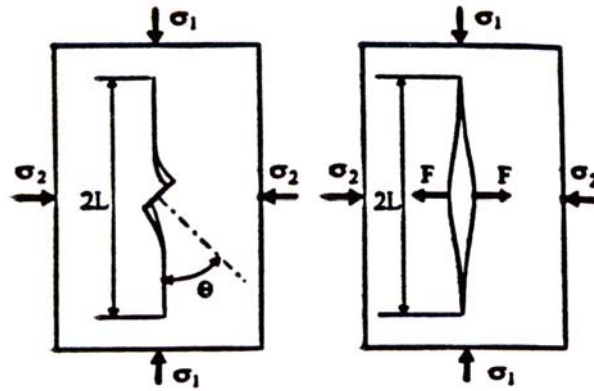


Figure 5.3. Simplified Crack Model (After Li and Nordlund, 1993)

The length of the growing crack has the following relation with the applied stresses:

$$L = 1/2\pi [((K_{IC}^2 + 2\sigma_2 F)^{1/2} - K_{IC}) / \sigma_2] \quad (\text{Eq. 5.1})$$

where, K_{IC} is the tensile fracture toughness. F is expressed as:

$$F = a_0 [(\sigma_1 - \sigma_2) g(\theta, \phi) - 2\sigma_2 \cos\theta \tan\phi] \quad (\text{Eq. 5.2})$$

where, $g(\theta, \phi) = (1 + \cos 2\theta)(\sin\theta - \cos\theta \tan\phi)$, a_0 is the half-length of the pre-existing crack, θ the orientation of the pre-existing crack and ϕ is the friction angle on the crack surface.

5.2 Kaiser Effect Mechanism based on the Fracture Model

Li (1998) used the fracture model concept to examine the mechanism of the Kaiser effect for three cases: (1) Uniaxial pre-loading and reloading in the same direction, (2) Uniaxial pre-loading and reloading in a different direction, and (3) Biaxial pre-loading and uniaxial reloading in the direction of σ_1 . Each of these three cases will be considered in the following sections.

Case (1): Uniaxial Pre-loading and Reloading in the Same Direction

When a rock specimen is loaded uniaxially, background AE occurs at an approximately constant level until the stress reaches σ_{11} , (see Figure 5.4(a)) at which level the wing cracks are initiated at the tips of the existing cracks. These wing cracks

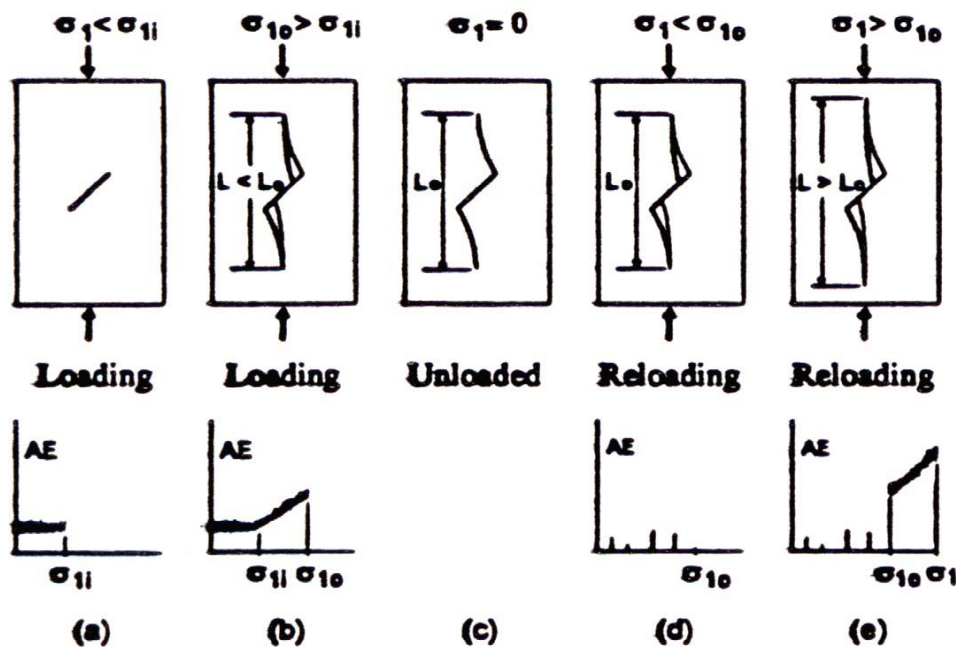


Figure 5.4. Sketches Showing the Fracture and AE under Uniaxial Loading and Reloading (After Li, 1998).

propagate with an increase in the applied load, resulting in increased AE (See Figure 5.4(b)). If the specimen is unloaded at a stress level σ_{10} , the corresponding length of the

propagated wing crack is L_0 . (See Figure 5.4(c)). During reloading, wing cracks do not grow and continuous AE does not occur till stress level σ_{10} is reached. (See Figure 5.4(d)). For higher stresses the propagation of wing cracks is resumed with an associated enormous increase in AE. This is the Kaiser effect. (See Figure 5.4(e)). Only a single crack oriented in the direction of loading has been analyzed, but Li (1998) adds that for a number of cracks oriented in different directions, the only variation would be the length of the crack, which would then become a function of the angle of orientation.

Case (2): Uniaxial Pre-loading and Reloading in a Different Direction

Supposing that there are wing cracks initiated at the tips of an inclined pre-existing crack under stress σ_1 , see Figure 5.5(a). The wing cracks tend to grow in the direction of application of σ_1 . The specimen is loaded to a specific stress level, it is unloaded to zero stress and then reloaded in a direction different from that of σ_1 , see Figure 5.5(b).

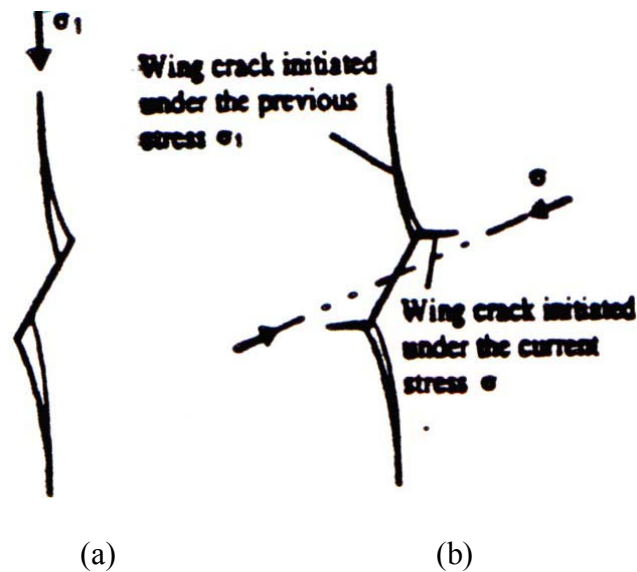


Figure 5.5 (a) Wing Cracks Under σ_1 . (b) New Wing Cracks Induced by σ , Applied in a Direction Different from σ_1 (After Li, 1998).

If the angle between the current loading stress σ and that of σ_1 is large enough, then, the wing cracks originally generated due to σ_1 will not grow under the current stress σ . It is, however, possible that σ will generate new wing cracks associated with the current loading direction (Figure 5.5(b)). The AE-onset stress would then be σ and not σ_1 . This case shows that for the second loading direction, the Kaiser effect could not be utilized to obtain the previous stress. This clearly contradicts the work of many researchers, and emphasizes the fact that the stress paths have to be the same during loading and reloading in order to obtain the previous stress state from the Kaiser effect phenomenon.

Holcomb (1983) also discusses this problem where he considers loading and reloading directions are orthogonal. He observes that though the initial loading would have used up many possible crack sites, there would be many more suitable sites left. In fact, the population of sites unfavorably oriented for the first stress direction would be exactly those that required a stress orthogonal to the first direction. Possibilities are sites where shearing would occur at a large angle relative to the initial stress field and tensile sites which would require crack opening parallel to the initial stress field. Thus, applying a stress orthogonal to the original direction would cause crack propagation and acoustic emissions independent of the first loading. For intermediate directions in the plane defined by the two axes, the stress required to propagate cracks and produce acoustic emissions would be expected to vary smoothly between the levels established by loading along the axes.

Case (3): Loading is biaxial, while reloading is uniaxial in the direction of σ_1 .

The growth of wing cracks is still in the direction of σ_1 , even in the case of biaxial compression (see Figure 5.6(a)). When the wing cracks grow to a certain length, both σ_1 and σ_2 are taken off and the specimen is reloaded uniaxially in the direction of σ_1 (see Figure 5.6(b)). The driving force for the propagation of the wing crack is the central wedge force F . Under reloading conditions, the wing cracks would propagate only when the stress level corresponds to the previous state (σ_1, σ_2).

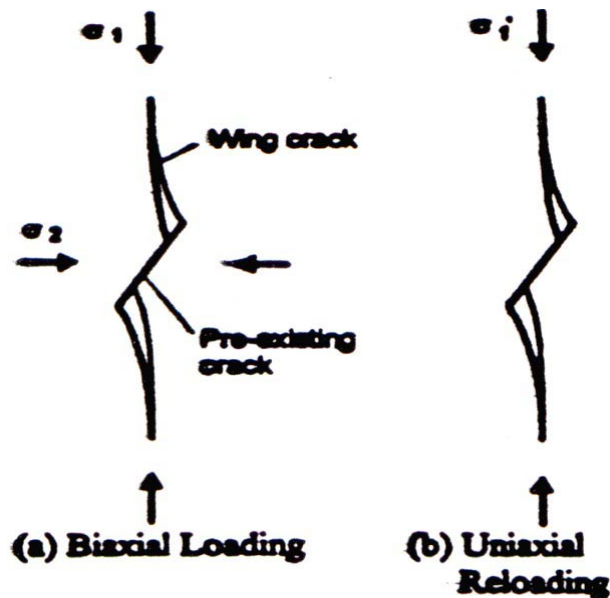


Figure 5.6. Wing Cracks Initiated by Biaxial Loading (a) and by Uniaxial Reloading (b). (After Li, 1998).

This is derived from Eq. (5.2), where the stress σ_{li} at which the wing cracks restart to grow, has the following relation with the previous stresses σ_1 and σ_2 :

$$\sigma_{li} = (\sigma_1 - \sigma_2) - \sigma_2 f(\theta, \phi) \quad (\text{Eq. 5.3})$$

where,

$$f(\theta, \phi) = \tan\phi / \cos\theta(\sin\theta - \cos\theta \tan\phi) \quad (\text{Eq. 5.4})$$

It is known that the normal and shear stresses on a pre-existing crack may be expressed as:

$$\sigma_n = (\sigma_1 + \sigma_2) / 2 + (\sigma_1 - \sigma_2) \cos 2\theta / 2 \quad (\text{Eq. 5.5})$$

$$\tau = (\sigma_1 - \sigma_2) \cos \theta / 2 \quad (\text{Eq. 5.6})$$

The effective shear stress on the pre-existing crack is calculated as:

$$\tau_{\text{eff}} = \tau - \sigma_n \tan \phi = (\sigma_1 - \sigma_2) \cos \theta (\sin \theta - \cos \theta \tan \phi) - \sigma_2 \tan \phi \quad (\text{Eq. 5.7})$$

Wing cracks will be re-initiated on the tips of the pre-existing crack when the effective shear stress satisfies the following relation:

$$K_{\text{IIC}} = \tau_{\text{eff}} (\pi a_0)^{1/2} \quad (\text{Eq. 5.8})$$

where K_{IIC} is the shear fracture toughness and a_0 is the half-length of the pre-existing crack. The differential stress for wing-crack initiation is obtained from Eq. (5.8) as:

$$(\sigma_1 - \sigma_2)_i = [K_{\text{IIC}} / (\pi a_0)^{1/2} + \sigma_2 \tan \phi] / \cos \theta (\sin \theta - \cos \theta \tan \phi) \quad (\text{Eq. 5.9})$$

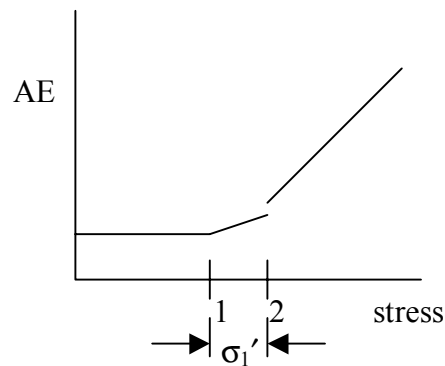


Figure 5.7. Ideal AE Record Under Uniaxial Reloading of a Biaxially Pre-loaded Specimen (After Li, 1998)

Zhang (1982) carried out a series of tests on triaxially pre-stressed specimens where $\sigma_2 = \sigma_3$, which is a case of biaxial loading. During uniaxial reloading it was found that a curve similar in form to Figure 2.16 was observed and Zhang assumed that the change in slope are associated with the Kaiser effect at the confining pressure (σ_2) and at the major

principal stress (σ_1). In contrast, Hughson and Crawford (1987) stated that the Kaiser effect depicts only the deviatoric stress or the stress differential ($\sigma_1 - \sigma_2$). Shen (1990, 1991) performed similar experiments and reported that the deviatoric stress and the major principal stress associated with the triaxial pre-loading are indicated by the Kaiser effect during uniaxial reloading of the specimen.

CHAPTER 6

DEVELOPMENT OF STANDARD TEST PROCEDURE

A detailed description of the development of a standard experimental procedure to study the Kaiser effect in Indiana Limestone and Cordova Limestone specimens and to evaluate a possible relationship between the pre-load stress and the reload stress is provided in this chapter. This procedure could be followed in future Kaiser effect studies. The author conducted some preliminary Kaiser effect tests. The tests to evaluate the Kaiser effect employ two loading cycles. In the first cycle the specimen is loaded to a specific stress level and then unloaded. In the second cycle, the specimen is loaded beyond the stress level achieved in the first cycle and an AE transducer is used to monitor and collect the observed AE data.

“Master” specimens (4 inches in diameter, 6 inches in length) were cored out of Indiana Limestone and Cordova Limestone blocks. The master specimens were then pre-stressed triaxially and smaller specimens (1.187 inches in diameter, 2.5 inches in length) were cored out of them at various orientations using a specially designed setup. Special end-caps were installed on the smaller specimens prior to the reloading cycle.

6.1 Test Material

The rock types chosen for this study were Indiana Limestone and Cordova Limestone. Though, Indiana Limestone is a very well understood material, not much of information was available on Cordova Limestone. Therefore, elastic strength tests were

conducted on Cordova Limestone specimens to determine its uniaxial compressive and tensile strengths and elastic moduli. The following table lists some of the physical properties of the rock types used for this study.

Physical Property	Indiana Limestone	Cordova Limestone
Uniaxial Tensile Strength (psi)	350-650	200
Uniaxial Compressive Strength (psi)	4000	2000
Young's Modulus (psi)	4.36×10^6	0.936×10^6
Poisson's Ratio	0.28	0.30

Table 6.1. Physical Properties of Indiana Limestone and Cordova Limestone

6.2 Specimen Preparation

By nature, rocks are hard and brittle. This leads to many difficulties in the process of accurate preparation of rock specimens. During the Kaiser effect tests, highly uniform loading surface is required which requires a very high degree of specimen quality. Special care has to be taken to prevent even the slightest damage to the rock specimens during coring, cutting and grinding operations.

Suitable dimensions for the test specimens were to be determined prior to specimen preparation. Zhang (1982) had worked on the Kaiser effect in the PSU-RML and his earlier test results seemed to be very successful. Hence, the author decided to adopt the same specimen dimensions used earlier by Zhang, namely: small specimens: $d = 1.187$ in. and $l = 2.5$ in., and master specimens: $d = 4$ in. and $l = 6$ in. The various stages of specimen preparation including coring, cutting, grinding, end-cap installation are described in the following sections.

6.2.1 Coring - As described earlier, two types of specimen coring were carried out in this study. Master specimen cores were drilled from square blocks of Indiana Limestone and Cordova Limestone, originally cut from the quarry and shipped to the PSU-RML. The drilling machine used, manufactured by the Milwaukee Electric Tool Corp., Brookfield, Wisconsin, was capable of operating at speeds of 375-750 RPM and had a vertical range of 2.5-8.0 inches. The diamond-core barrels used were, for the master specimens type R144.2, Revcore PS-48 and for the smaller specimens, type R1.460, Revcore PS-74, both manufactured by Hoffman Diamond Products, Punxsutawney, Pennsylvania.

A view of the set-up used for coring the master specimens is shown in Figure 6.1A. During coring, the drilling machine was mounted on a concrete platform. The rock block being cored was held in place tightly by two post clamps attached to a steel frame also mounted on the concrete platform to prevent it from rotating or vibrating during

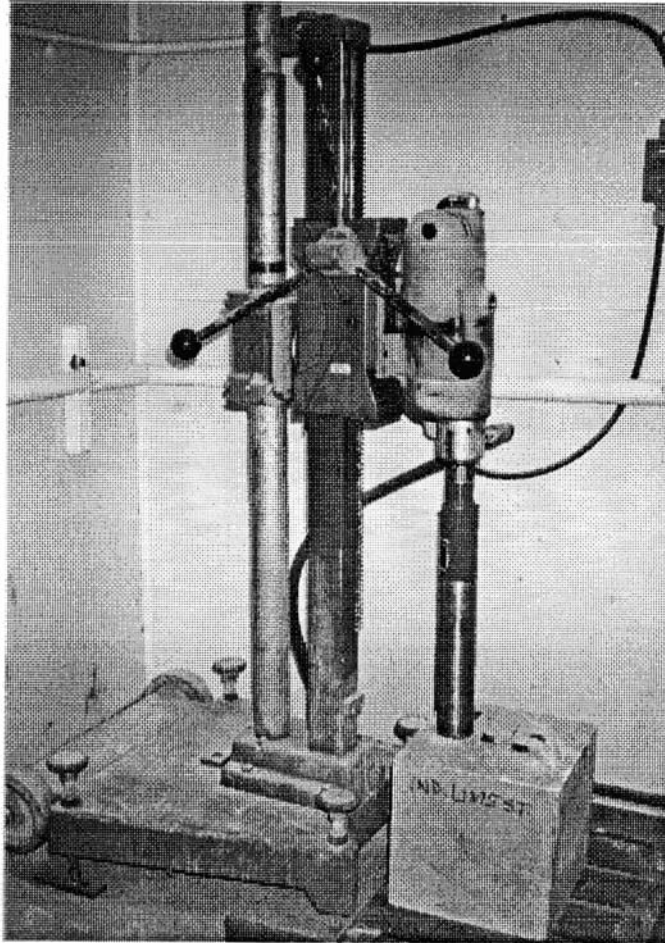


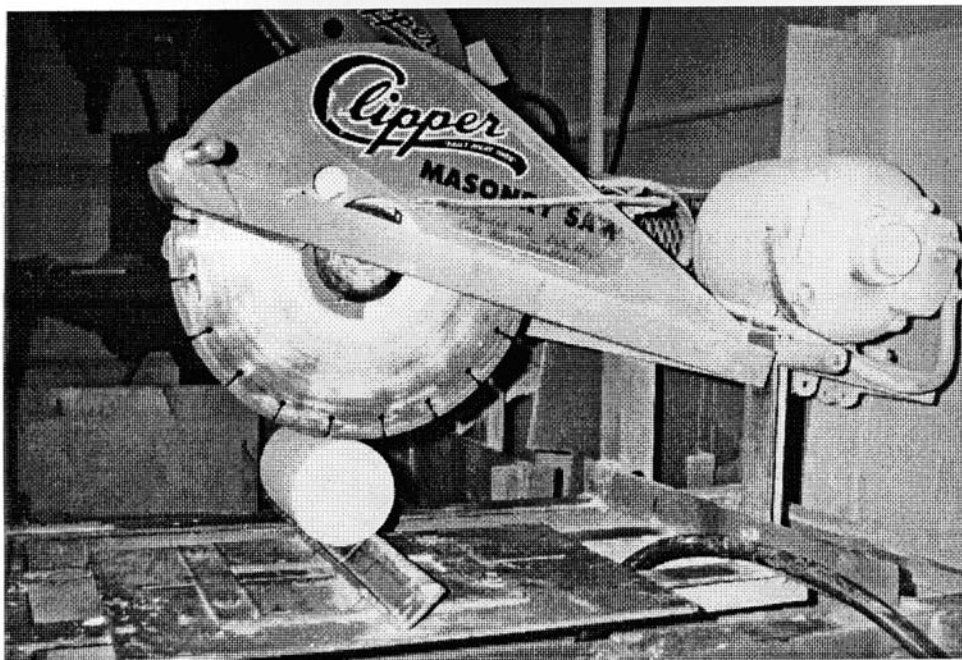
Figure 6.1. Preparation of Cores Using a Diamond Drill

drilling. The operation speed of the drilling machine was 375 RPM and the feed was controlled manually. The manual feed had to be kept as uniform and steady, as possible to generate a smooth core surface. Water was used as the coolant during coring.

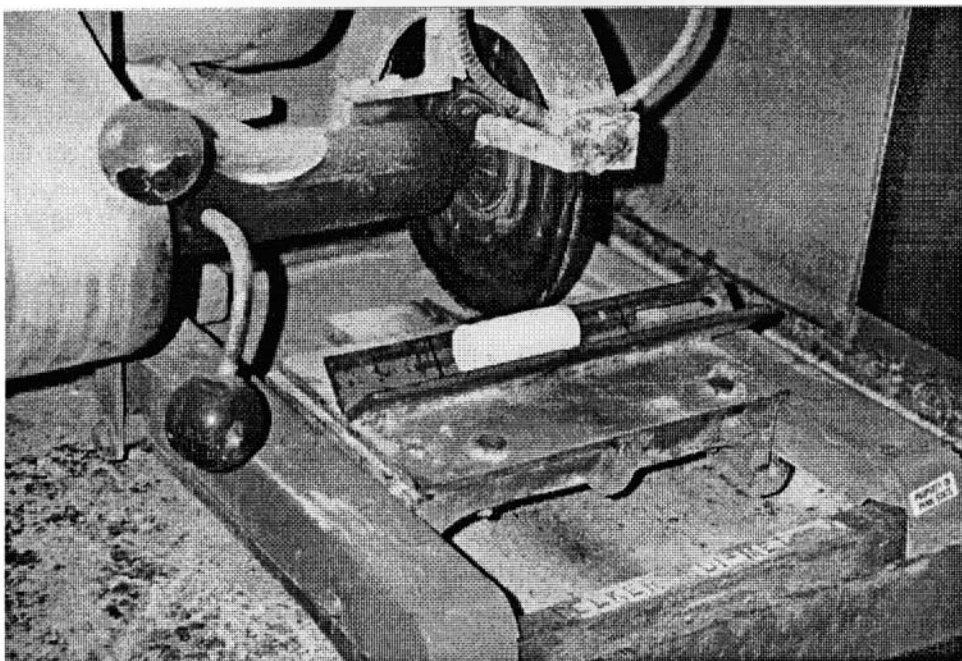
For coring smaller specimens at various orientations from the master specimens, a special wooden drilling set-up was designed in the PSU-RML. The drilling set-up enabled coring of smaller specimens at angles of 0° , 45° , 60° and 90° respectively, to the vertical axis of the master specimen. The drilling set-up was fixed to the steel frame using nuts and bolts. The groove that holds the master specimen could be articulated to be set at

various desired angles. Once again, the feed was manual and extreme care was taken to ensure smooth core surface.

6.2.2 Cutting -The cores drilled earlier were then cut to an approximate length of 2.5 in. for smaller specimens or 6 in. for the master specimens. The master specimen cores were cut using a Clipper Masonry Saw, Model HD50, manufactured by the Clipper Company, Kansas City, Missouri, operated at a shaft speed of 3500 RPM. A 14-in. diameter, diamond-impregnated blade manufactured by the same company was used. The core was held by a V-channel support welded to the lower platen of the saw during cutting. The core was held firmly by hand while the saw was operating to prevent any vibration. Special care was taken to prevent chipping of the specimen edges by slowly advancing the blade at the beginning and end of the cutting operation. Water was used as the coolant during the cutting operation. An overall view of the set-up is shown in Figure 6.2A. The saw used for cutting the smaller specimens was basically similar to the one used for master specimens. It was a Felker Di-Met saw, Model 11B, manufactured by the Felker Manufacturing Company, Torrance, California (Figure 6.2B). A 4-in. diamond-impregnated blade was used. As usual, water was used as the coolant during the cutting operation.



(A) Saw Used for Large Core.



(B) Saw Used for Small Core.

Figure 6.2. Diamond Saws Used for Cutting of Master and Smaller Specimens

6.2.3 Surface Grinding -The next stage in the process of specimen preparation was to grind the two ends of each specimen. The grinder used was a model 618 Micromaster Surface Grinder Machine, manufactured by the Brown & Sharp Co., Providence, Rhode Island. It uses a carborundum grinding wheel for this purpose.

The specimen was held in a V-block by two clamps during the grinding operation. Care had to be taken not to tighten the clamp screws too much so as to prevent the damaging of the circumferential surface of the specimen. The incremental grinding depth was 0.005 in. for rough cuts and 0.002-0.001 in. for the final cuts. An overall view of the surface grinder set-up is shown in Figure 6.3.

6.2.4 End-Cap Installation - During AE studies in rock specimens under compression, the friction between the loading platens and the rock specimen causes end-effects as well as generates random AE activity. To resolve this problem, a suitable adhesive “hunch” or “end-cap,” made of Araldite epoxy resin and cement mixture (1:1.5 by weight) was attached to both of the loading ends of the specimens by Kanagawa et al. (1976). In later studies, Zhang (1982) at Penn State, made the end-cap from a mixture of cement (Portland) and Devcon “2-ton” epoxy with a ratio of 1:1 by weight and had shown that it worked excellently in reducing the end-noise. Therefore, the author used the same mixture for fabricating the end-caps in this study.

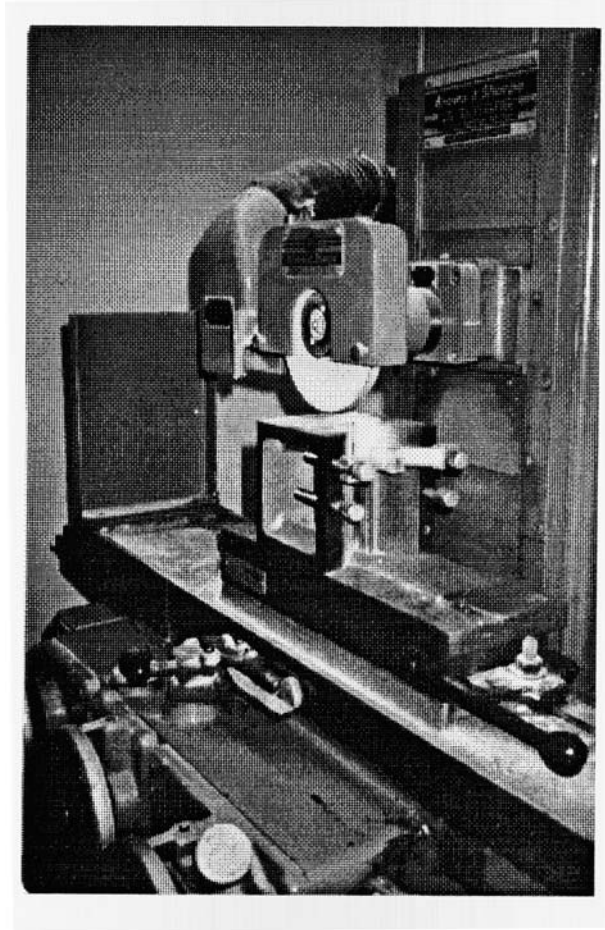


Figure 6.3. Overall View of the Surface Grinder Set-up.

Though, the AE characteristics of the end-cap material and the effectiveness of the end-caps in reducing random AE activity have been studied in considerable detail, the effect of the presence of an end-cap on the stress and displacement distributions during the loading of the rock specimens have not been examined. Therefore, the author carried out an independent study to develop a Finite Element (FE) model of an end-capped rock specimen and analyze the stress distributions and the variations of displacement due to the application of compressive load. FE studies were carried out on Indiana Limestone,

Cordova Limestone and Barre Granite. The elastic moduli of the end-cap material were not available in literature and hence, tests were carried out to determine them.

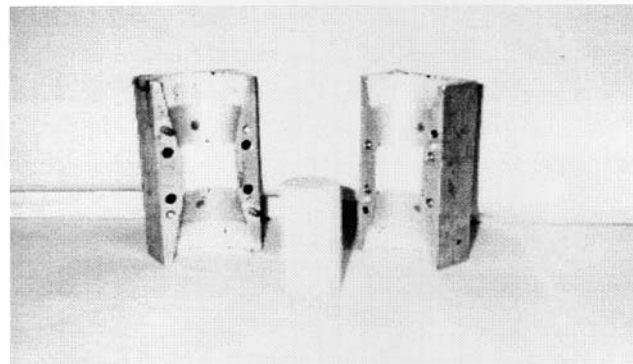
The details of the independent study (Jayaraman, 2000) are not provided here but the important conclusions are listed below:

- (a) The Young's modulus and Poisson's ratio values of the end-cap material were found out to be 0.495×10^5 psi and 0.44, respectively.
- (b) The stress distributions in the end-capped rock types investigated, for all practical purposes, could be considered as uniform.
- (c) The mid-section stress values experienced by the end-capped rock specimens are very close to the applied stress. Therefore, the presence of the end-cap does not effectively alter the stress values in the central section of the rock specimen.
- (d) The displacement distribution plots for all the three rock types investigated were found to be close to those expected.
- (e) Devcon "2-ton" epoxy and Portland cement mixture (1:1 by weight) is ideal for the fabrication of specimen end-caps for use in Kaiser effect tests.

End-caps were installed only on the smaller specimens. Figure 6.4A shows the mold and the associated specimen. A thin metal strip was wrapped around the center portion of the rock specimen before the specimen was placed in the mold, to hold the specimen firm in its proper position during the end-cap molding process. A dry spray lubricant, "Elmer's Slide-All" manufactured by the Borden Inc., Columbus, Ohio, was applied to the inner wall of the mold, especially the inner wall of the cone-shaped section to assist in removing the specimen from the mold after the end-caps are installed. The two mold pieces are assembled, held in place by screws so that there was no gap visible between

the two parts (Figure 6.4B). For each end-cap, 8 grams of Devcon epoxy and 8 grams of Portland cement were used. These were mixed in a paper cup and a small stick was used to stir the mixture. The mixture was then poured into one end of the mold, as shown in Figure 3.4 B, and the mold was set on a stable, horizontal plane. The curing time for the mixture is 8 hours and therefore, after one end is cured, the mold is inverted for the installation of the end-cap on the other end of the specimen.

After the epoxy at both ends had cured, the specimen could be removed from the mold. The four retaining screws were removed first. The four mold opening screws were rotated slowly to separate the specimen from the mold.



(A) Specimen and the Mold Used.



(B) Material Used for the End-Cap.

Figure 6.4. Details Associated with End-cap Installation

6.2.5 Lathe Operations -The end surfaces of the end-capped specimen were ground to insure the specimen ends were plane-parallel and smooth. A Clausing Lathe, Model 5907, manufactured by Clausing Company, Kalamazoo, Michigan, and an attached tool-post grinder were used for this operation. A pair of collets clamped to the center section of the specimen was then held by a three-jaw chuck for automatic centering. When the chuck was tightened, care was taken to ensure the specimen was held firmly by the chuck, i.e. the circumferential surface of the clamped end of the collets should be in total contact with the inner surface of the chuck jaws. Figure 6.5 shows the specimen in place on the lathe, ready for end smoothing.

The grinding parameters used were as follows:

(a) Rough cuts:

Lathe speed 280 RPM

Carriage transverse speed 0.003 in./rev.,

Depth of cut 0.05 in.

(b) Finishing cuts

Lathe speed 280 RPM

Carriage transverse speed 0.003 in./rev.,

Depth of cut 0.005 in.

Figure 6.6 shows a specimen with its ends ground and ready for AE tests.

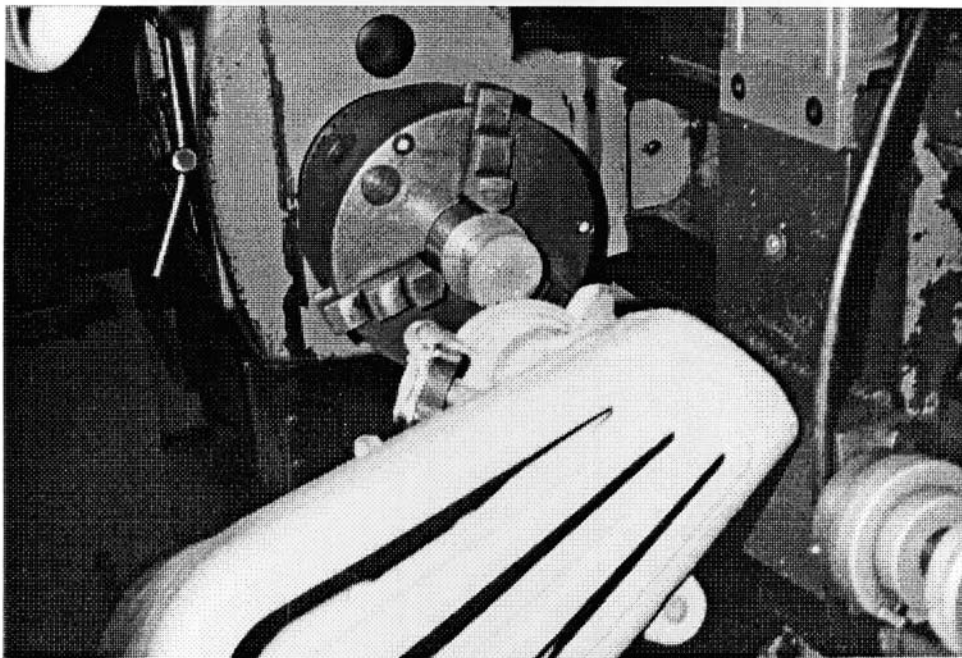


Figure 6.5. Specimen Located in Lathe Ready for Grinding.

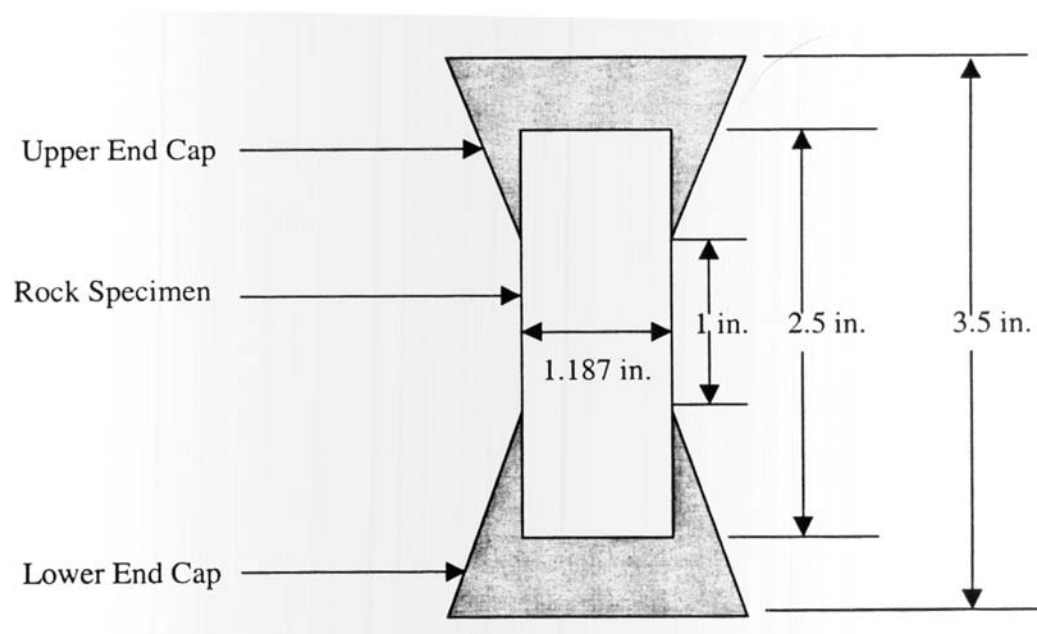


Figure 6.6. Rock Specimen with End-Caps Showing Dimensions

6.3 Pre-Stressing of Master Specimens

The Indiana Limestone and Cordova Limestone master specimens were loaded to a pre-determined stress level triaxially. The pre-stress levels for both the rock types were same and were determined taking into consideration the compressive strengths of the rock types investigated and the maximum capacity of the loading machine. A case of uniaxial pre-loading was also done.

6.3.1 Triaxial Pre-Stressing of Master Specimens - A Baldwin 60000-lb Compression testing machine was used to provide the axial stress (σ_1) on the master specimens. Oil was pumped into a triaxial loading vessel to provide the confining pressure ($\sigma_2 = \sigma_3$). The vertical stress and confining pressure combinations used for triaxial pre-stressing of the master specimens are listed in Table 6.2.

	Axial Load (lbs)	Axial Stress (psi)	Confining Pressure (psi)
A	12560	1000	0
B	12560	1000	200
C	12560	1000	400

Table 6.2 Axial Stress and Confining Pressure Combinations for Triaxial Pre-Stressing

Figure 6.7 shows the specimen loading arrangement for triaxial pre-stressing. The master specimen was inserted in a rubber jacket and was placed on the base of a special loading head. The top of the special loading load was then placed on the specimen (Figure 6.8). The interface between the specimen and the special loading heads were taped so as to prevent the damaging of the thin rubber jacket while building up the confining pressure in the triaxial vessel by pumping oil. The thin rubber jacket which was cut to size (approximately should extend from top of the loading head to the base loading head) using a razor knife on a wooden board, was then slipped on to the set-up. The interface between the O-ring seal and the rubber jacket was then taped, both at the top and the bottom.

The screw head on the outer frame of the triaxial vessel was taken off before the outer frame was raised to a certain height using chains connected to the top loading platen of the compression machine. The outer frame was raised to a height enough to accommodate the loading heads with the specimen, which were then, placed on the base of the triaxial vessel.

The outer frame was then lowered onto the base. Screws on the outer frame were used as a guide to the place the outer frame on the base. The system was now seated in such a way that the oil inlets point exactly between the two posts of the compression machine and are parallel to the special arrangement made for drawing external strain gage connections. Screws were then tightened to seal the outer frame with the base. The screw head was then placed and tightened using a special wrench and the loading piston was finally placed. Brass and Teflon disks were placed between the loading piston and the upper platen of the compression machine to achieve higher load uniformity.

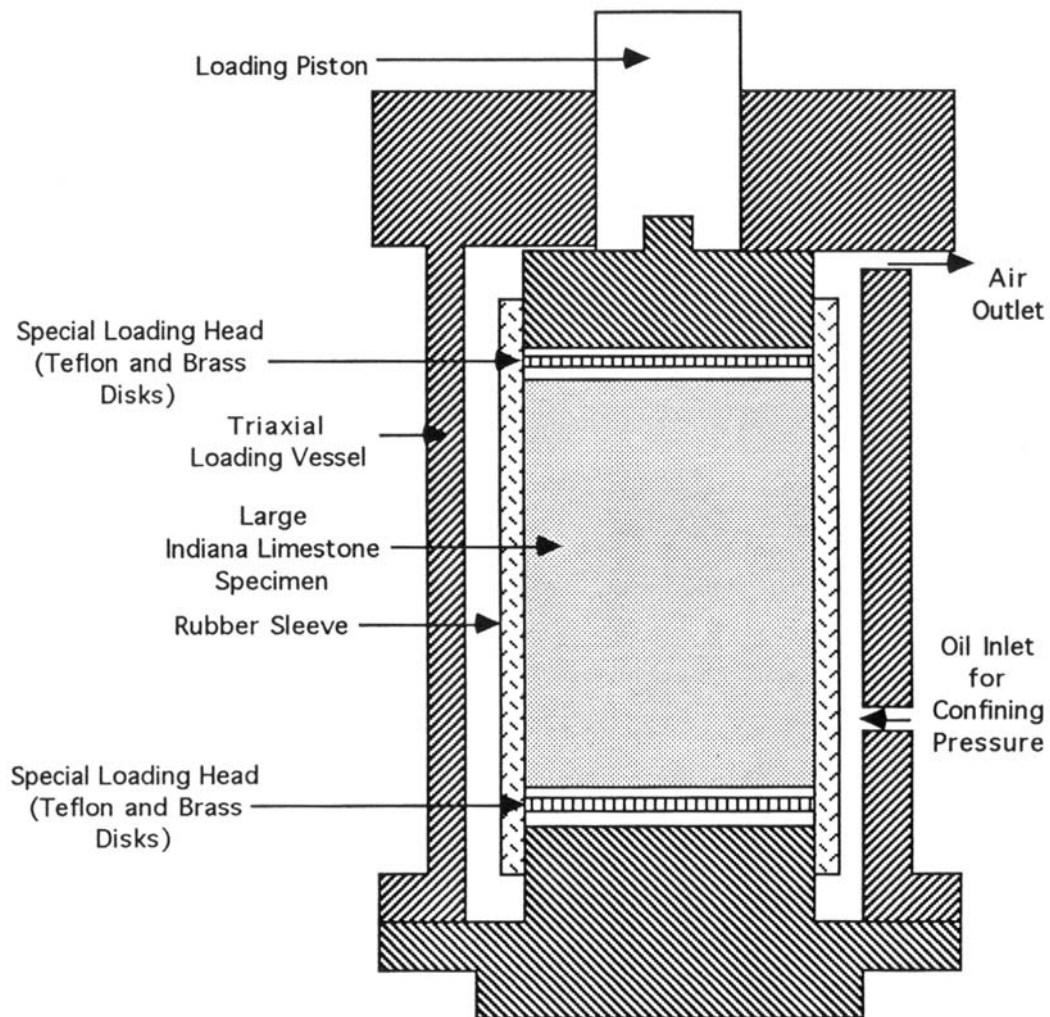


Figure 6.7 Loading Arrangement for Triaxial Pre-Stressing of Master Specimens

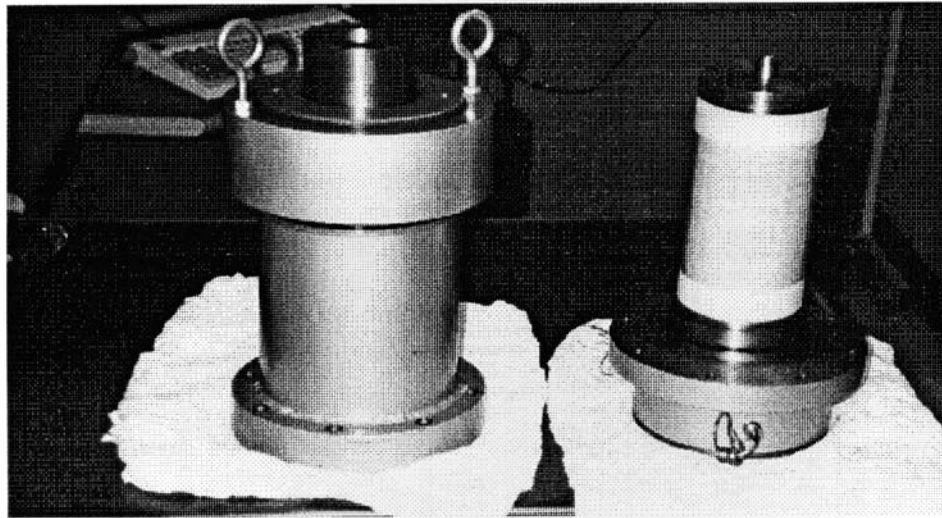


Figure 6.8. Triaxial Vessel (left) and Master Specimen Placed on the Triaxial Cell Base (right).

Figure 6.9 depicts the plumbing arrangements required to pump oil into the triaxial vessel as well as to drain it out. The oil pump was connected to the oil inlet of the triaxial vessel through a high-pressure valve (V1) and a pressure gage. The air outlet of the triaxial vessel was connected to the laboratory air supply through a high-pressure valve (V2) and two other low-pressure valves (V3 and V4). While pumping oil into the triaxial vessel, V1, V2 and V3 were kept open initially and V4 closed. The “selector valve” of the pump was twisted to the “to lift” position and the “release valve” of the pump was kept closed. As soon as oil started filling up in the vessel, some of it flowed out through V3 where the oil was collected in a beaker. Now, V2 and V3 were closed and the system was ready to be loaded.

The compression machine was then turned on to load the system. An attempt was made to ensure that the difference between the axial stress and the confining pressure was not great, so as to prevent the development of high shear stresses in the master

specimens. The maximum axial load and confining pressure used were 12560 lbs, and 200 psi, respectively. Initially, the axial load was taken to 3000 lbs and the confining pressure to 50 psi. Later, the axial load was taken to 6000 lbs and the confining pressure to 100 psi. In a similar manner, the maximum axial load and confining pressure were achieved and were held for 30 minutes so as to “freeze” the stresses in the rock specimen. Once the desired confining pressure was reached, V1 was closed to hold the pressure.

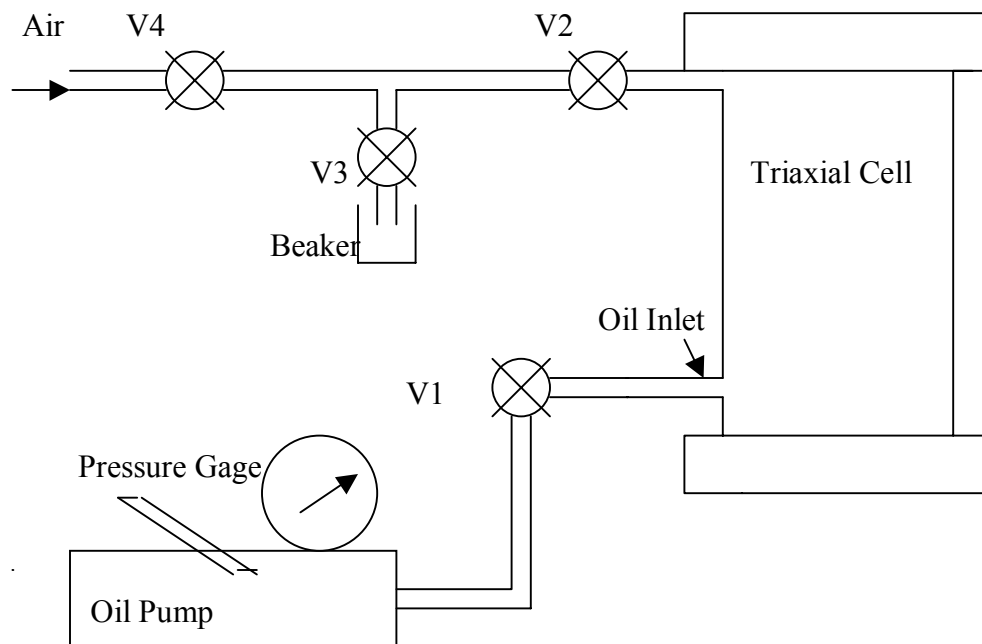


Figure 6.9. Plumbing Arrangement to Provide Confining Pressure During Triaxial Pre-Stressing of Master Specimens.

After the “hold” period, the stresses were taken down by the same step-by-step procedure. During unloading, the “selector” valve was kept closed and the “release” valve was kept open to allow the flow of oil back into the pump. V1 and V2 were kept

open and so was V4 to let the air in and push the oil back into the pump. While draining the oil, the oil tank was kept open to hear the entry of air into the tank, which indicated that most of the oil had been drained out. After most of the oil had been drained, the screws were loosened and the outer frame of the triaxial vessel was raised using the chains tied to the upper platen of the compression machine. The rubber jacket was cut open and the specimen was pushed out of the rubber sleeve.

6.3.2 Uniaxial Pre-Stressing of Master Specimens -The uniaxial pre-stressing is a special case of triaxial pre-stressing where the confining pressure is zero. Figure 6.10 shows the specimen loading arrangement for uniaxial pre-stressing. Suitable metal end-caps were chosen. Brass disks and Teflon disks were inserted between the specimen and the end-cap. The arrangement was then placed on a hemispherical block on the lower platen of the Compression testing machine. The brass disks, Teflon disks and the hemispherical block aid in achieving uniform loading and compensate for any non-parallelity between the specimen end surfaces. The axial load was slowly increased to 12560 lbs (1000 psi) and held for 30 minutes. The specimen was unloaded after the “hold” period.

After the master specimens have been pre-stressed, smaller test specimens are cored out of them at different angles. End-caps are applied on these smaller specimens. The various steps involved in the preparation of the test specimens have described in detail at the start of this chapter. The test specimens are reloaded, the AE data is collected and the Kaiser stress is determined.

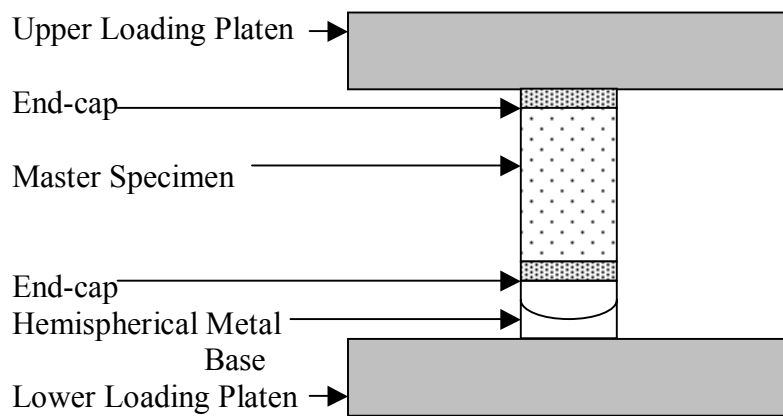


Figure 6.10. Loading Arrangement for Uniaxial Pre-Stressing of Master Specimens.

CHAPTER 7

DISCUSSION

The Kaiser effect method is a widely used technique for the determination of in-situ stress in the laboratory. Researchers earlier had postulated that the AE-onset stress during the uniaxial reloading of a rock core extracted from a geologic structure is indicative of the in-situ stress in that direction. From all the theoretical analysis shown earlier, it is very clearly perceptible that this approach to determining the in-situ stress may have serious drawbacks.

There is no clear demarcation that the AE-onset stress depicts the prevailing stress or the previous maximum stress. Suppose, a landslide occurred over an area. The landslide would generate very large dynamic stresses on the geologic structures beneath it. After the landslide, the geologic activity in the area would return to normal. Now, the static load over that area would primarily be due to the overburden. If a rock core were extracted from that area, what would the AE-onset stress indicate? The prevailing stress or the previous maximum dynamic stress due to the landslide? More studies will have to be conducted to completely understand this phenomenon.

In its virgin state, any geologic structure is acted upon by triaxial stresses. Therefore, the AE-onset stress during the uniaxial reloading of a specimen core extracted from that geologic structure would reflect the triaxial stress configuration rather than the stress in the reload direction.

A standard experimental procedure for conducting the Kaiser effect tests was developed. Some preliminary tests were also conducted. Future Kaiser effect tests in

rocks may be conducted using this procedure. The pre-load stress combinations to be used in the laboratory should be chosen wisely so that they exceed the stress-state the rock specimen was under, in the field. This would ensure a definite occurrence of the Kaiser effect in the rock specimen and enhance the possibility of arriving at the right conclusions.

The choice of rock type to be used in these tests to develop a relationship between the pre-load stresses and the Kaiser stress should be made very carefully. Rock types such as Cordova Limestone that inherently possess acoustic damping properties due to their geologic origin, should be avoided, if possible. It is the author's opinion that rock types like Sandstone and Granite are very suitable for these experiments.

The various methods utilized to determine the Kaiser stress from the experimental data also have an important bearing on the final result. An accepted standardized procedure should be put in place.

After the Kaiser stress has been determined from the experimental data, it will then have to be correlated to the pre-load stresses, namely, the axial stress and the confining pressure. Li (1998) has analyzed the triaxial stress state configuration theoretically and this should be utilized as a guideline in the future Kaiser effect tests.

There is a wide variety of commercially available software that could be used in the curve-fitting procedure. The Kaiser stress will have to be plotted against the pre-load stress, confining pressure, deviatoric stress, angle at which the smaller AE test specimens were cored, elastic properties of the rock specimen tested etc. The empirical relationships could be deduced from the plots.

REFERENCES

1. Boyce, G.L. (1981), "A Study of the Acoustic Emission Response of Various Rock Types", Master of Science Thesis, Drexel University, Philadelphia.
2. Bombolakis, E.G. (1963), "Photo-elastic Stress Analysis of Crack Propagation, within a Compressive Stress Field", Ph.D. Thesis, Massachusetts Institute of Technology.
3. Brace, W.F. (1965), "Some New Measurements of Linear Compressibility of Rocks", *Journal of Geo-Physical Research*, Vol.70, No.2, pp. 391-398.
4. Brace, W.F. and E.G. Bombolakis (1963), "A Note on Brittle Crack Growth in Compression", *Journal of Geo-Physical Research*, Vol.68, No.12, pp. 3709-3713.
5. Goodman, R.E. "Sub-audible Noise during Compression of Rocks", *Geological Society of America Bulletin*, Vol. 74, pp. 487-490.
6. Haimson, B.C. (1974), "A simple Method for Estimating In-Situ Stresses at Great Depths," *American Society of Testing Material, Spec. Tech. Publ.*, pp. 156-182.
7. Hardy, H.R., Jr., (1981), "Applications of Acoustic Emissions to Rock and Rock Structures: A State-of-the-Art Review," Acoustic Emissions in Geotechnical Engineering Practice, STP 750, ASTM, Philadelphia, pp. 4-92.
8. Hardy, H.R., Jr., (1985), Theory and Application of Acoustic Emission/Microseismic Techniques, Transtech Publications, Clausthal, Germany.
9. Hardy, H.R., Jr., (1989), Fourth Conference on Acoustic Emission/Microseismic Activity in Geologic Structures and Materials, Proceedings of Conference held at Pennsylvania State University, October 1985, TransTech Publications, Clausthal, Germany, 711 pp.
10. Hardy, H.R., Jr., (1995), Fifth conference on Acoustic Emission/Microseismic Activity in Geologic Structures and Materials, Proceedings of Conference held at Pennsylvania State University, June 1991, TransTech Publications, Clausthal, Germany, 755 pp.
11. Hardy, H.R., Jr., and H.W Shen (1992), "Recent Kaiser effect studies in rock," Progress in Acoustic Emission VI, The Japanese Society for NDI, pp. 149-157.
12. Hayashi, M. (1979), "Acoustic Emission to Detect Geo-stress," Discussion paper in Thema 2, Proceedings of the Fourth International Congress for rock Mechanics, Montreux, Vol. 3.

13. Holcomb, D.J. (1983), "Using Acoustic Emissions to determine In-situ stress: Problems and Promise," *Geomechanics AMD Vol. 57*, Ed. S. Nemat-Nasser, Pub. ASME, 1983.
14. Hughson, D.R., and A.M. Crawford (1986), "Kaiser Effect Gauging: A New Method for Determining the Pre-Existing In-situ Stress from an Extracted Core by Acoustic Emissions," *Proceedings International Symposium on Rock Stress and Rock Stress Measurements*, Stockholm, Sweden, 1-3 September 1986, pp. 359-368.
15. Hughson, D.R., and A.M. Crawford (1987), "Kaiser effect gauging: The influence of confining stress on its response," *Proceedings of the sixth International congress for Rock mechanics*, Montreal, Canada, pp.981-985.
16. Jayaraman, S. (2000), "Study of the Effect of End-Cap on Stress Distribution in Rock Specimens in Compression," Internal Report RML-IR/00-1, Rock Mechanics Laboratory, Department of Energy and Geo-Environmental Engineering, Pennsylvania State University.
17. Kaiser, J. (1953), "Erkenntnisse and Folgerungen aus der Messung Von Gerauschen bei Zugbeanspruchung von Metallischen Werkstoffen," *Archiv Fur das Eisenhüttenwesen*, Vol. 24, pp. 43-45.
18. Kanagawa, T., M. Hayashi, and H. Nakasa (1976), " Estimation of spatial geostresses in rock samples using the Kaiser effect of Acoustic emission," *Proceedings Third Acoustic Emission Symposium*, Tokyo, Japan, 1976, pp. 229-248.
19. Kurita and Fujii (1979), "Stress memory of some crystalline rocks in Acoustic Emission," *Geophysical Research Letters*, Vol. 6, No. 1, pp. 9-12.
20. Leeman, E.R. (1969), "The 'Doorstopper' and Triaxial Rock Stress measuring Instruments Developed by CSIR,' *Journal of the South African Institution of Mining and Metallurgy*, Vol. 69, pp. 305-339.
21. Leeman, E.R. and D.J. Hayes (1966), "A Technique for Determining the Complete State of Stress Using a Single Borehole," *Proceedings, First Congress of the International Society of Rock Mechanics*, Lisbon, Vol. 2, pp. 17-24.
22. Li, C. and E. Nordlund (1993), "Experimental Verification of Kaiser Effect in Rocks," *Rock Mechanics and Rock Engineering*, Vol. 26, No. 4, pp. 333-351.
23. Li, C. (1998), "A Theory for the Kaiser Effect in Rock and Its Potential Applications", *Proceedings Sixth Conference on AE/MS Activity in Geologic Structures and Materials*, Pennsylvania State University, June 1996, TransTech Publications, Clausthal, Germany, pp. 187-194.

24. Lord, A.E., Jr., and R.M. Koerner (1985), "Field determination of pre-stress (Existing stress) in soil and rock masses using Acoustic emission," Proceedings Second International Conference on Acoustic Emission, Lake Tahoe, Nevada, October/November 1985, Journal of Acoustic Emission Supplement, pp. S11-S16.
25. Michihiro, K., T. Fujiwara, and H. Yoshioka (1985), "Study on estimating geostress by the Kaiser effect of AE," Proceedings 26th US Symposium on Rock Mechanics/ Rapid City, SD/June 1985, pp. 557-564.
26. Michihiro, K., H. Yoshioka, K. Hata, and T. Fujiwara (1989), "Strain dependence of the Kaiser effect for various rocks," Proceedings Fourth Conference on AE/MS Activity in Geologic Structures and Materials, Pennsylvania State University, October 1985, TransTech Publications, Clausthal, Germany, pp.87-95.
27. Momeyez, M., F.P. Hassani, and H.R. Hardy, Jr (1992), "Maximum Curvature Method: A Technique to estimate Kaiser-Effect load from Acoustic Emission data," Journal of Acoustic Emission, Vol. 10, No. ¾, pp. 61-65.
28. Obert, L. and W.I. Duvall (1967), "Rock Mechanics and the Design of Structures in Rock", John Wiley & Sons, Inc.
29. Shen, H.W. (1990), "Kaiser effect experiments-Report No. 1," Internal Report RML-IR/90-3, Rock Mechanics Laboratory, Department of Mineral Engineering, Pennsylvania State University, 181 p.
30. Shen, H.W. (1991), "Kaiser effect experiments-Report No. 2," Internal Report RML-IR/91-6, Rock Mechanics Laboratory, Department of Mineral Engineering, Pennsylvania State University, 69 p.
31. Shen, H.W. (1992), "Laboratory Studies of the Kaiser effect in Rock", Master of Science thesis, Pennsylvania State University, 194p.
32. Shen, H.W., (1993), "Objective Kaiser stress evaluation in rock," Proceedings Fifth Conference on AE/MS Activity in Geologic Structures and Materials, Pennsylvania State University, June 1991, TransTech Publications, Clausthal, Germany, pp. 177-196.
33. Yoshikawa, S., and K. Mogi (1981), "A new method for estimation of the crustal stress from cored rock samples: Laboratory study in the case of uniaxial compression," Tectonophysics, Vol. 74(1981), pp. 323-339.
34. Zelanko, J.C. (1983), "Determination of in-situ stresses using Acoustic Emission techniques-A literature review," Internal Report RML-IR/83-7, Geomechanics Section, Department of Mineral Engineering, Pennsylvania state University, 30 p.

35. Zhang, D.L. (1982), "Use of Kaiser effect for estimation of the previous state of stress in rock," Internal Report RML-IR/82-4, Geomechanics Section, Department of Mineral Engineering, Pennsylvania State University, 39 p.